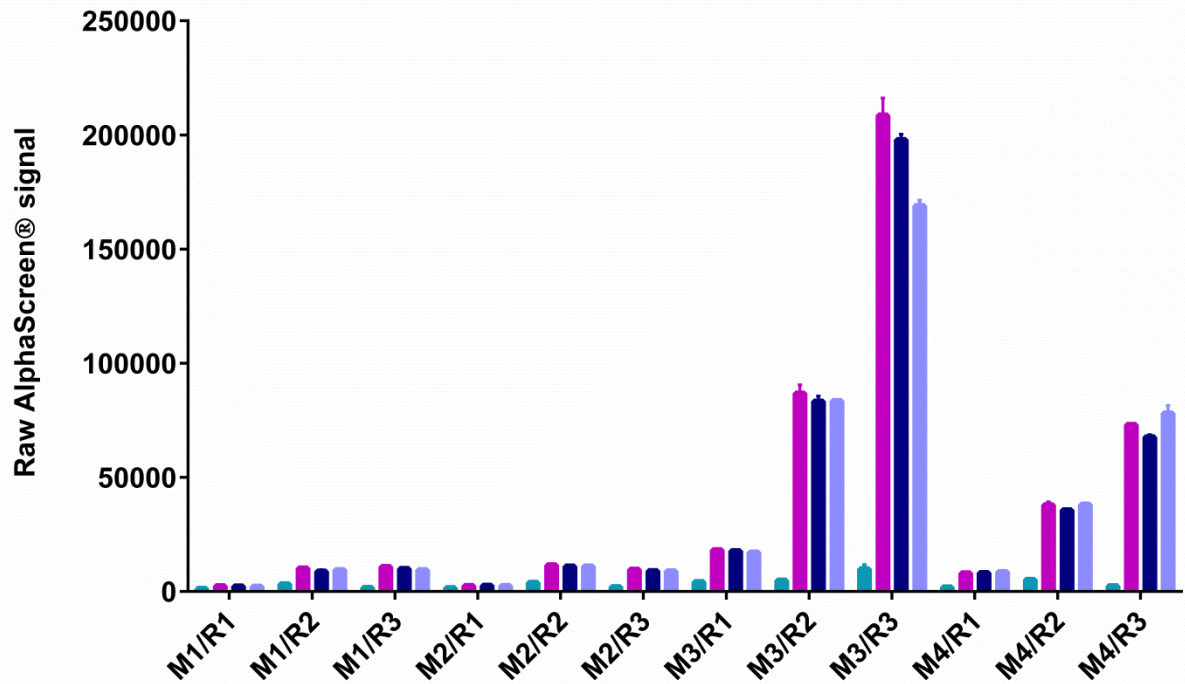


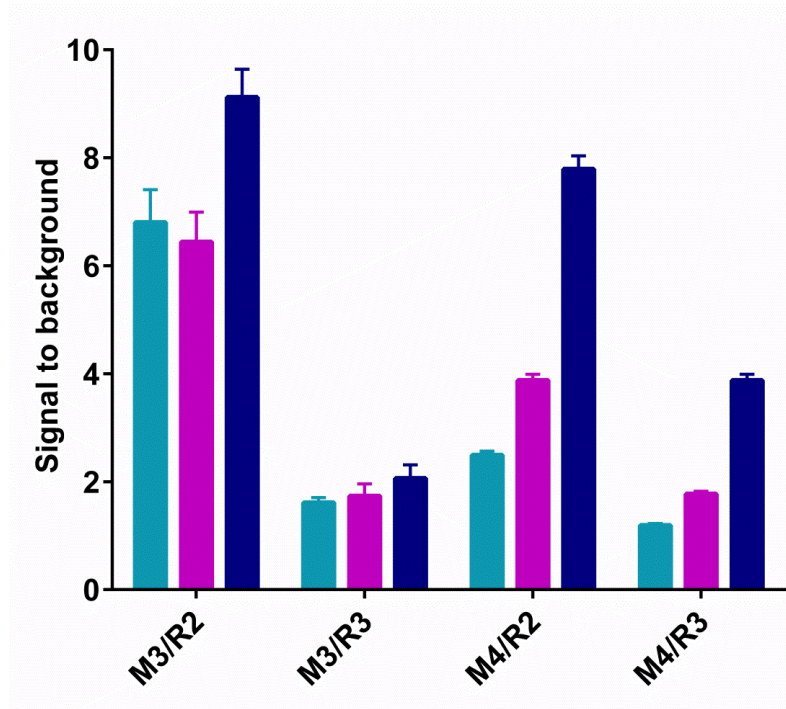
**Supplementary Figure 1| Schematic outline of the assay principle for the AlphaScreen® assay used to detect human thymidylate synthase in cell lysates.**

Detection requires dual simultaneous recognition of native folded thymidylate synthase. This was achieved using antibodies from two different species, in this case from mouse (yellow) and rabbit (purple). Commercially available antibodies directed towards thymidylate synthase were efficiently screened using AlphaScreen® acceptor and donor beads functionalized with capturing antibodies recognizing the Fc domain of IgG antibodies from these two species (see Supplementary Table 1 for an overview of the antibodies included in this study). Singlet oxygen transfer between the donor and acceptor beads occurs only when the two bead types are close in space. This occurs when a productive complex involving the following components is formed in solution:

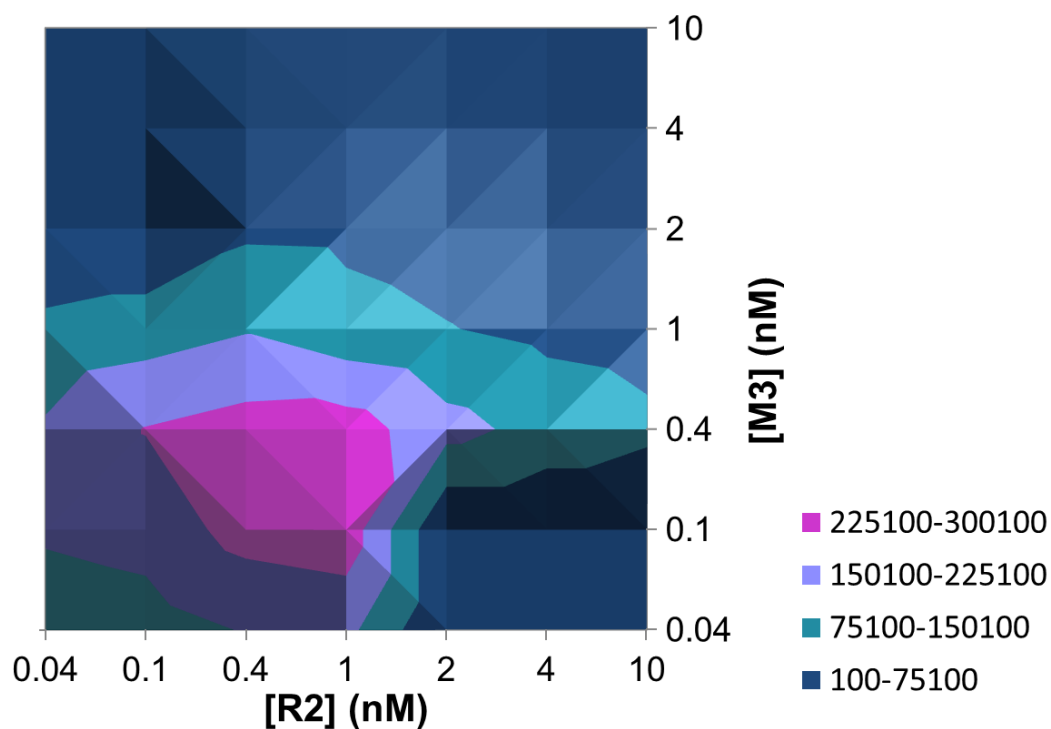
- Donor beads conjugated with an antibody recognizing the Fc domain of mouse derived antibodies
- Mouse derived antibody recognizing thymidylate synthase
- Thymidylate synthase
- Rabbit derived antibody recognizing thymidylate synthase
- Acceptor beads conjugate with an antibody recognizing the Fc domain of rabbit derived antibodies



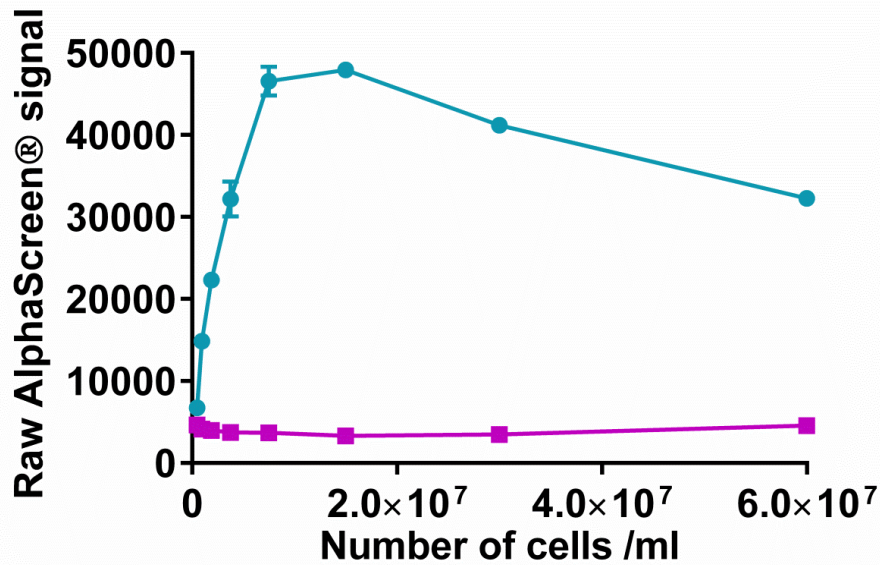
**Supplementary Figure 2| Results from screening of antibody pairs for dual recognition of recombinant thymidylate synthase using AlphaScreen®.** All possible combinations of four mouse-derived (M1-M4) and three rabbit-derived antibodies (R1-R3) recognizing different epitopes of thymidylate synthase (Supplementary Table 1) were tested. Four different conditions were included for each pair, with two of those being the absence (green) and presence of 2 nM of thymidylate synthase (magenta). Given our previous experience of ligand induced quenching of protein target recognition by the antibody pair (Jafari *et al.*, 2014) we also included a control containing 100 μM deoxyuridine monophosphate (dUMP) (blue) and a control containing 100 μM dUMP and 10 μM raltitrexed (lavender blue). Data are provided as the average and range from experiments done in duplicate at one independent test occasion. Four tentatively suitable pairs were identified and further testing was required for selection of the most appropriate pair.



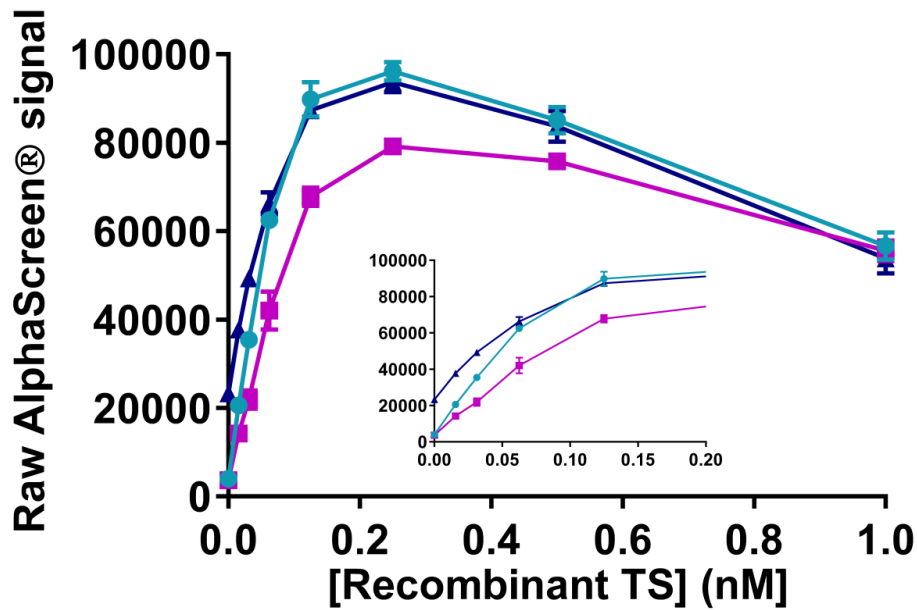
**Supplementary Figure 3| Illustration of the kinetics for recognition of thymidylate synthase in cell lysates from K562 cells in the AlphaScreen® assay.** Four different antibody combinations were selected for testing based on the results of the experiment in Supplementary Fig. 2. The experiment was performed to address the ability of the four different antibody pairs to recognize thymidylate synthase also in the context of cell lysates. Establishment of an equilibrium signal that remains stable over several hours is essential to allow parallel processing of multiple plates in screening campaigns. For each tested pair the signal to background is given as a function of time after addition of antibodies and beads: 2h (green), 6h (magenta) and 18h (blue). Data are provided as the average and standard error of mean from experiments done in triplicate at one test occasion. Based on the combination of an excellent signal to background and a comparatively fast and stable recognition of thymidylate synthase also in the context of the cell lysates we decided on a pair based on the mouse M3 and the rabbit R2 antibodies (Supplementary Table 1) for further assay development purposes.



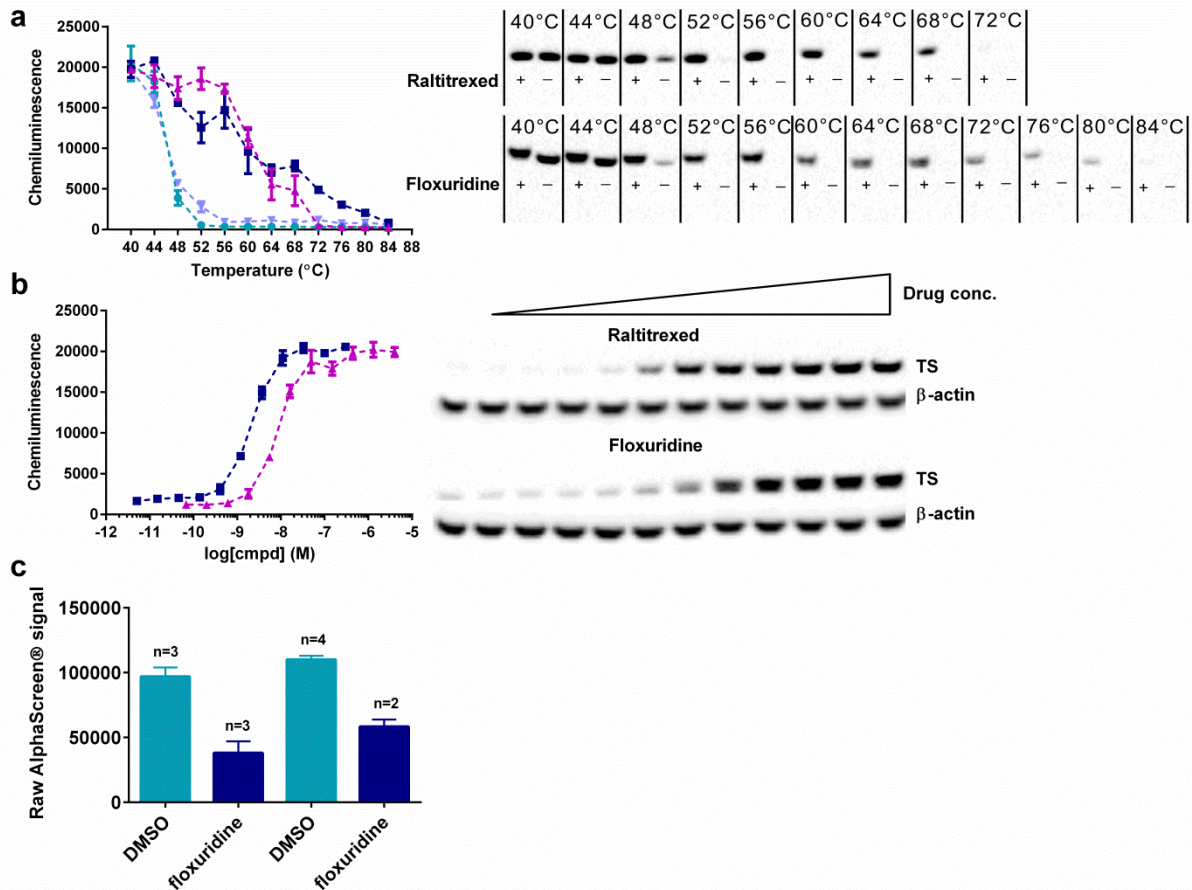
**Supplementary Figure 4| Illustration of the AlphaScreen® response for thymidylate synthase as a function of antibody concentrations.** Given that a multi-component complex must be formed to yield a productive assay signal (see Supplementary Fig. 1 for an illustration of the assay principle) the antibody concentrations must be titrated to avoid hook effects in the assay. Data are shown as a 3D contour graph where the concentrations of the antibodies directed towards thymidylate synthase are varied on the x-axis (R2) and y-axis (M3), respectively (see Supplementary Table 1 for details on the antibodies). The experiment was done based on a cell lysate from 7.5 million K562 cells per mL. Data are provided as the average from experiments done with  $n=2-4$  for each condition obtained at one test occasion. Based on these results we decided to use 0.4 nM M3 and 1.0 nM R2 in the final screening assay.



**Supplementary Figure 5| Illustration of the AlphaScreen® signal for human thymidylate synthase as a function of K562 cell numbers.** For assays measuring the content of soluble protein it is important to work in a range where the signal responds linearly with the cell numbers. Data are shown as the average and standard error of mean from triplicate samples obtained at one test occasion. Labels are as follows: cell lysate from cells kept at room temperature (green circle) or after heating to 52°C for 3 minutes (magenta square). This transient heat treatment denatures and precipitates thymidylate synthase in these cells (Fig. 1b in main text). In order to maximize the signal window without the risk of saturating the detection system we decided to use 5 million K562 cells per ml in the final screening assay.



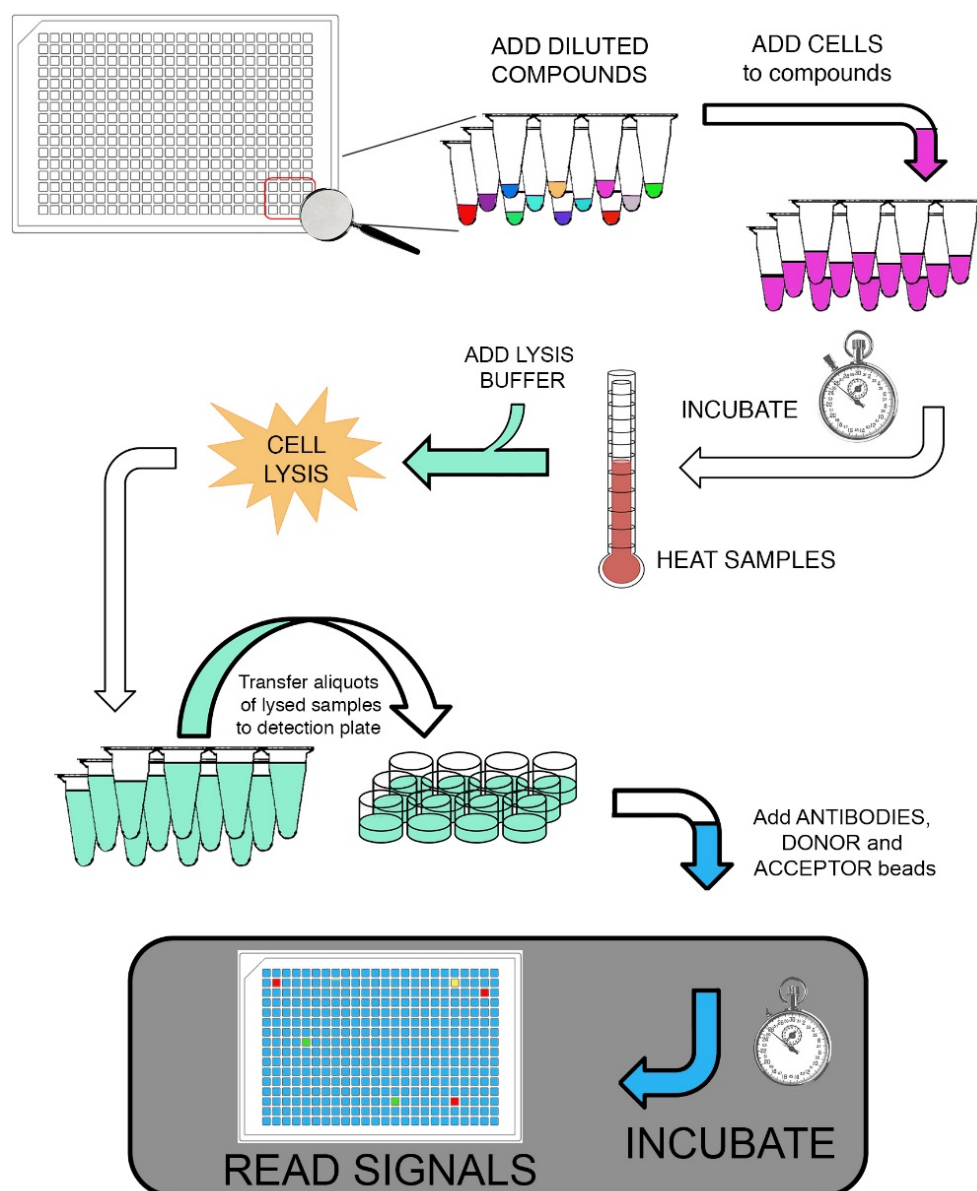
**Supplementary Figure 6| Illustration of the change in AlphaScreen® signal as a function of added recombinant thymidylate synthase to K562 cell lysates.** To address the specificity of the selected dual antibody pair (M3 and R2; Supplementary Table 1) for recognition of human thymidylate synthase in the context of a complex cell lysate we performed seeding experiments with thymidylate synthase added to unheated cell lysates (blue triangle), lysates heated to 52°C for 3 minutes (magenta square), or to cell medium without any cells (green circle). The insert illustrates the same data, but restricted to the 0-0.2 nM concentration range. Data are shown from one test occasion as the average and standard error of mean (S.E.M) from triplicate samples. To stay within the linear range of the assay response the cell lysate background corresponded to 1 million K562 cells per ml. Although the background levels in the absence of TS are different for the unheated lysate, reflecting the TS levels in the K562 cells, there is a corresponding increase in the signal in both lysates, whereas the signal increase is somewhat steeper in the absence of the cell lysate background. Based on these data we conclude that the signal scales with thymidylate synthase content also in the cell lysates.



**Supplementary Figure 7 | Comparison of Western blot and AlphaScreen® based responses for floxuridine and raltitrexed.** (a) Western blot data from CETSA experiments performed to determine  $T_{agg}$  curves for thymidylate synthase in live cells following a 2h preincubation period in the presence of DMSO (green circle and lavender blue downwards triangle) and 5  $\mu$ M floxuridine (blue square) or 5  $\mu$ M raltitrexed (magenta upwards triangle). To the right of the graphs are the corresponding chemiluminescence data. (b) Western blot based ITDRF<sub>CETSA</sub> following a 2h preincubation period at 37°C at different concentrations of floxuridine (starting at 300 nM and serially diluted in 11 steps down to 5 pM) (blue square) and raltitrexed (starting at 4  $\mu$ M and serially diluted down to 67 pM) (magenta upwards triangle) and after heating for 3 minutes at 50°C. To the right of the graphs are the corresponding chemiluminescence data probing TS as well as the corresponding  $\beta$ -actin levels. All Western blot experiments were performed on K562 cells at a minimum of two independent biological replicates. (c) Illustration of the AlphaScreen® response in lysates from K562 cells for DMSO (green bars) and floxuridine treated cells (blue bars). Data are shown as the average and S.E.M. for two independent biological replicates following a 2h pre-incubation period. While Western blot experiments demonstrate similar protein levels between controls and treated samples (see panel a), we consistently observed a significant attenuation (~50%) of the AlphaScreen® signal for fluoropyrimidines. Intracellular enzymatic conversions of the fluoropyrimidines generate the active species FdUMP that forms a ternary covalent complex with thymidylate synthase and 5,10-methylenetetrahydrofolate (see panel

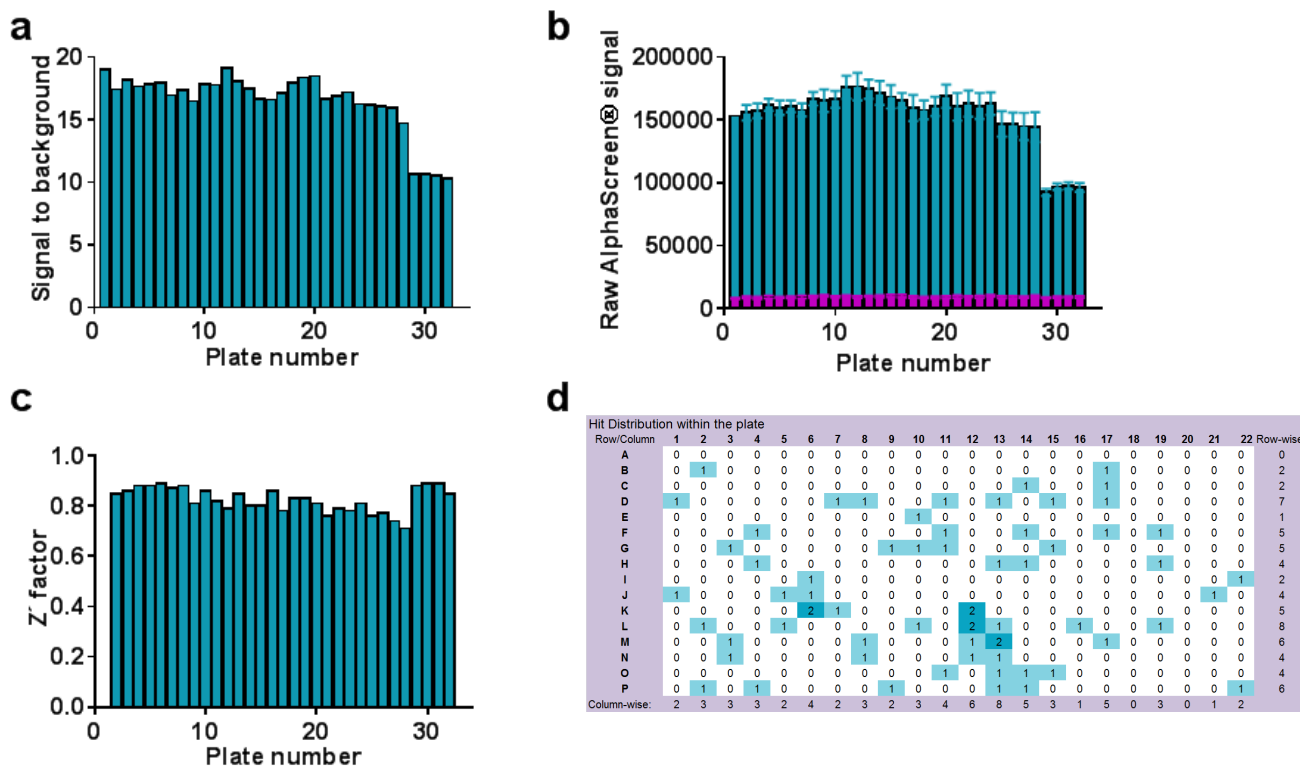
**a** for a characteristic shift in electrophoretic mobility of the ternary complex)<sup>1</sup>. As previously reported<sup>2</sup>, we commonly observe ligand induced attenuation of the AlphaScreen signal® in the no-wash assay setup because the ligand is present also during detection. Despite the observation of signal attenuation for a small number of covalently binding compounds in this case we proceeded with the selected antibody pair and assay setup since it resulted in excellent assay performance.



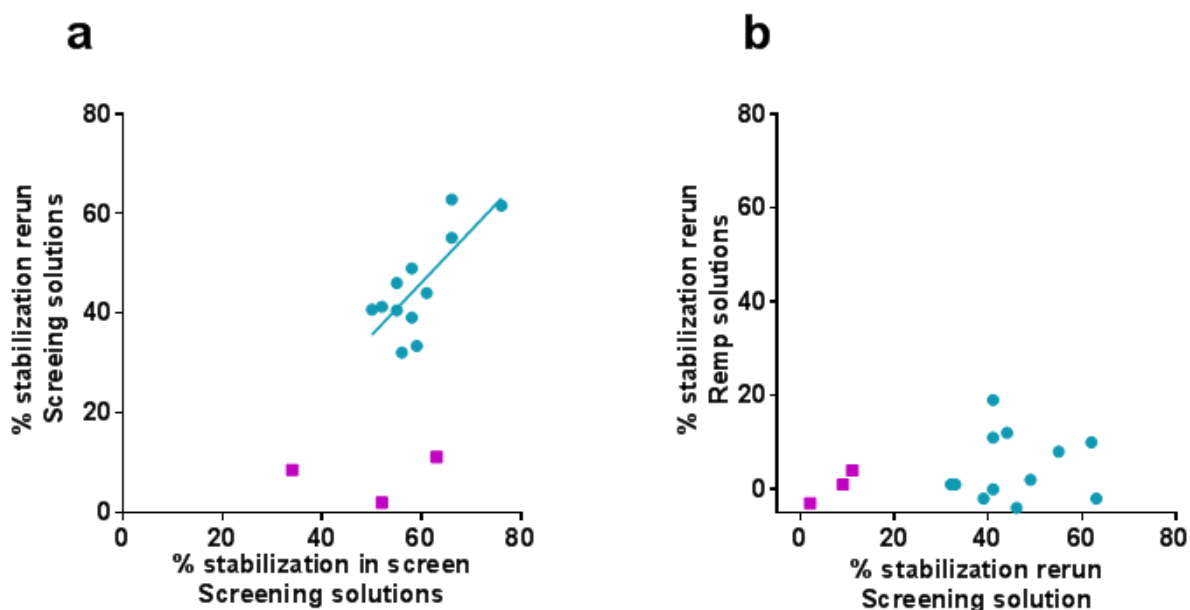


**Supplementary Figure 8| Schematic outline of the small molecule screening logistics applied in the screening campaign on human thymidylate synthase using CETSA.**

Compounds and controls were dispensed to round-bottomed 384-well plates using an Echo 550 and diluted with supplemented cell medium using a Multidrop Combi. The diluted compounds were next transferred to 384-well PCR plates using a Bravo liquid handling station. K562 suspension cells were then added using a multipipette followed by preincubation for 2h in a cell incubator at 37°C. The PCR plates were next heated transiently to 50°C for three minutes followed by a controlled cooling to 20°C using a Roche Lightcycler480. The plates were then centrifuged briefly and subsequently cell lysis was accomplished by addition of lysis buffer using a Flexdrop IV. To ensure sufficient lysis the cell lysates were thoroughly mixed by ten repetitions of aspirations and dispenses using the 384-well head of the Bravo. Part of the lysates were then transferred to white 384-well plates followed by the addition of antibodies and AlphaScreen® acceptor and donor beads using a Multidrop Combi under subdued light. The plates were incubated over night at room temperature prior to detection in an Envision plate reader. As described in the Methods section the plates were sealed under several of these steps.



**Supplementary Figure 9| Illustration of the primary screening results using CETSA to measure target engagement of human thymidylate synthase in K562 cells. (a)** Signal to background based on controls for each individual 384-well plate included in the screening campaign. The values were calculated based on averages of 16 each of negative (0.5% DMSO; column 23) and positive controls (100 nM raltitrexed; column 24). **(b)** Signal and background of the measured AlphaScreen® responses for the controls on each screening plate. Data are shown as the average and S.E.M. **(c)** Calculated Z' factors based on negative and positive controls on each individual 384-well plate. **(d)** Illustration of the distribution of hits identified in the primary screen, *i.e.* the plate well location for solutions demonstrating more than 11.7% stabilization of human thymidylate synthase.



**Supplementary Figure 10| Additional testing on compound solutions that did not reproduce activity in the first hit confirmation experiment.** Several hits resulting in >30% apparent stabilization in the primary screen did not confirm activity when they were retested as a function of compound concentration (highlighted at the bottom of Supplementary Table 3). A key difference between these experiments was the use of different sources for the compound solutions. Whereas the screen was based on compound solutions plated from Labcyte 384 LDV plates, the hit confirmation experiment was based on compound solutions taken directly from a vial based storage system at CBCS. Additional experiments on these two sets of compound solutions were hence performed to investigate whether the CETSA screen was associated with a poor hit confirmation rate or whether there were different activities observed in the two sets of compound solutions. **(a)** Correlation between the responses observed in the primary screening campaign (single replicate) and a follow-up experiment based on solutions from the same Labcyte 384 LDV compound source plates (illustrated as the average of a duplicate obtained at one test occasion). Out of 15 tested solutions 12 reproduced significant activity (green circle) with a correlation coefficient of 0.56 between the two experiments, whereas three solutions failed to reproduce activity (magenta square). **(b)** Comparison of activities observed on solutions taken from the Labcyte 384 LDV compound source plates on the x-axis versus those prepared from the REMP vial storage system on the y-axis (in both cases illustrated as the averages of duplicate measurements obtained at one test occasion). Regardless of whether the hits reproducibly showed activity (green circle), or not (magenta square), when tested from the source plates that were applied in the primary screening campaign they failed to demonstrate activities approaching 30% stabilization when tested based on the REMP vial solutions. The source plates were generated by tip based transfer of solutions from the REMP-based vials to the compound

plates using a 96-well head and these solutions were then moved further with a 384-well head into 1536-well plates. In both these transfers the tips were washed extensively with DMSO between vials and plates. Despite these precautions careful inspection of the laboratory notes describing the generation of the Labcyte 384 LDV plates demonstrates that five of the contaminated solutions had been in contact with a pipette tip that had transferred a 10 mM floxuridine solution in a preceding step, while another three repeatedly active solutions were adjacent to wells containing floxuridine. Based on these observations we concluded that the original source plates are cross-contaminated and generated new plates for future screening campaigns.

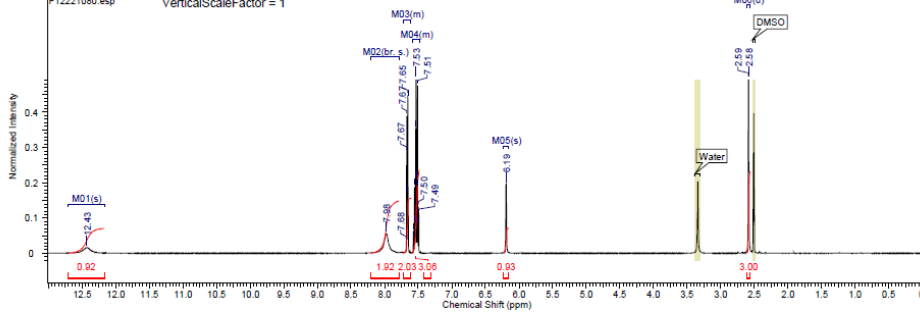
a

This report was created by ACD/NMR Processor Academic Edition. For more information go to [www.acdlabs.com/nmrproc/](http://www.acdlabs.com/nmrproc/)

2015-06-30 13:53:35

|                        |  |                        |   |
|------------------------|--|------------------------|---|
| Acquisition Time (sec) | 3.1654   | Comment                | Group LCBK11_F12221080_K11H_DMSO_IC18BrukerTopspin2181mahara 23 |
| Date                   | 29 Jun 2015 16:45:20   | Date Stamp             | 29 Jun 2015 16:45:20  |
| File Name              | \\130.229.43.168\ROD\local\Agneta\data\maharainm1506007410\data\111r | Frequency (MHz)        | 400.13  |
| Nucleus                | <sup>1</sup> H   | Number of Transients   | 16  |
| Owner                  | mnr  | Points Count           | 65536   |
| Sweepwidth (Hz)        | 10351.97   | Solvent                | DMSO-d6   |
| Sweep (Hz)             | 10351.81   | Temperature (degree C) | 23.300  |
|                        |  | Pulse Sequence         | zg  |
|                        |  | Spectrum Offset (Hz)   | 4801.2981   |
|                        |  | Receiver Gain          | 181.00  |
|                        |  | Spectrum Type          | STANDARD  |

<sup>1</sup>H NMR (400 MHz, DMSO-d<sub>6</sub>) δ ppm 2.58 (d, J=0.95 Hz, 3 H) 6.19 (s, 1 H) 7.48 - 7.59 (m, 3 H) 7.61 - 7.73 (m, 2 H) 7.98 (br. s., 2 H) 12.44 (s, 1 H)



| No. | (ppm)        | Annotation | Layer No. | Created By        | Created At           | Modified By | Modified At |
|-----|--------------|------------|-----------|-------------------|----------------------|-------------|-------------|
| 1   | [2.49, 2.53] | DMSO       | 1         | martin.haraldsson | 12015-08-30 08:02:45 |             |             |
| 2   | [3.31, 3.38] | Water      | 1         | martin.haraldsson | 12015-08-30 08:02:45 |             |             |

| No. | Shift (ppm) | Hz | Type   | J (Hz) | Multiplet | (ppm)          | No. | (ppm)    | Value      | Absolute Value | Non-Negative Value |
|-----|-------------|----|--------|--------|-----------|----------------|-----|----------|------------|----------------|--------------------|
| 1   | 2.58        | 3  | d      | 0.95   | M06       | (2.56, 2.61)   | 12  | 8504.268 | 0.0028052  | 8.28679552e+8  | 3.00028052         |
| 2   | 6.19        | 1  | s      | -      | M05       | (6.16, 6.23)   | 216 | 1570.022 | 0.92834902 | 2.55791792e+8  | 0.92834902         |
| 3   | 7.53        | 3  | m      | -      | M04       | (7.48, 7.59)   | 317 | 4781.758 | 0.05773424 | 8.42509962e+8  | 3.05773426         |
| 4   | 7.66        | 2  | m      | -      | M03       | (7.61, 7.73)   | 417 | 8074.772 | 0.28190114 | 5.68835520e+8  | 2.02819014         |
| 5   | 7.68        | 2  | br. s. | -      | M02       | (7.79, 8.20)   | 517 | 889.820  | 0.2180651  | 5.29523200e+8  | 1.92180657         |
| 6   | 12.44       | 1  | s      | -      | M01       | (12.17, 12.71) | 617 | 174.127  | 0.2178244  | 2.53982444e+8  | 0.62178243         |

b

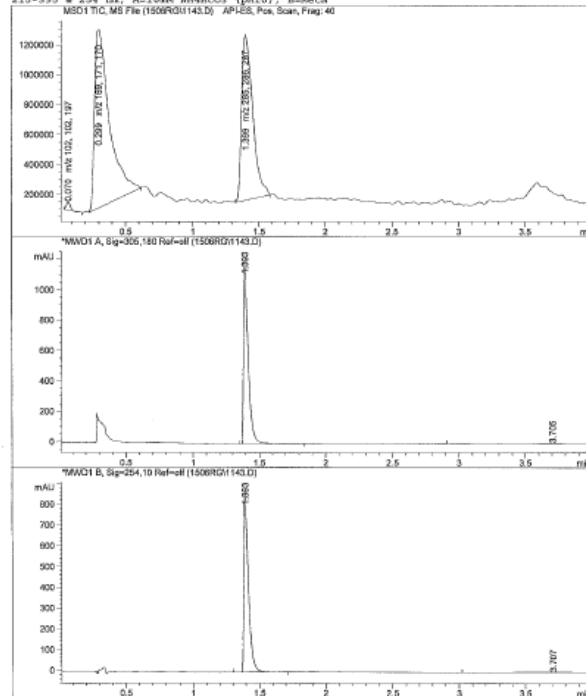
Data File C:\HPCHEM\1\DATA\1506RG\1143.D

Sample Name: CBK115334

F12221080

```

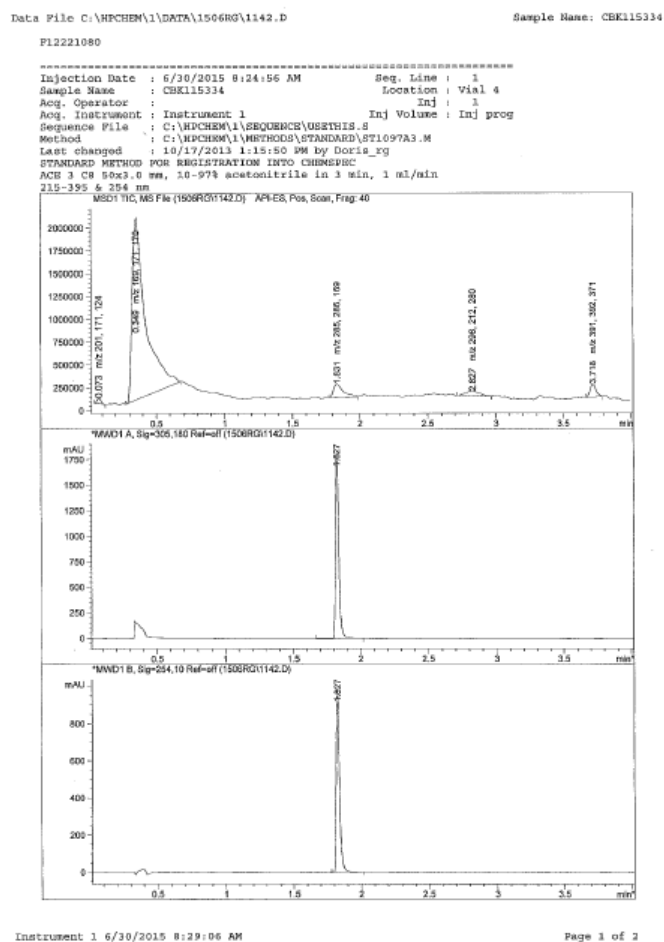
-----
Injection Date : 6/30/2015 8:31:09 AM          Seq. Line : 2
Sample Name    : CBK115334                    Location  : Vial 4
Acq. Operator  :                             Inj      : 1
Acq. Instrument: Instrument 1                 Inj Volume: Inj prog
Sequence File  : C:\HPCHEM\1\SEQUENCE\USETH18.S
Method         : C:\HPCHEM\1\METHODS\STANDARD\EX1097X1.M
Last changed  : 10/13/2013 1:29:39 PM by Doris_rg
STANDARD METHOD FOR IDENTIFICATION INFO CHEMSPEC
Xterra C18 50x3.0 mm, 10-97% acetonitrile in 3 min, 1 ml/min
215-395 & 254 nm, A=10nm NH4HCO3 [pH11.0], B=MeCN
  
```



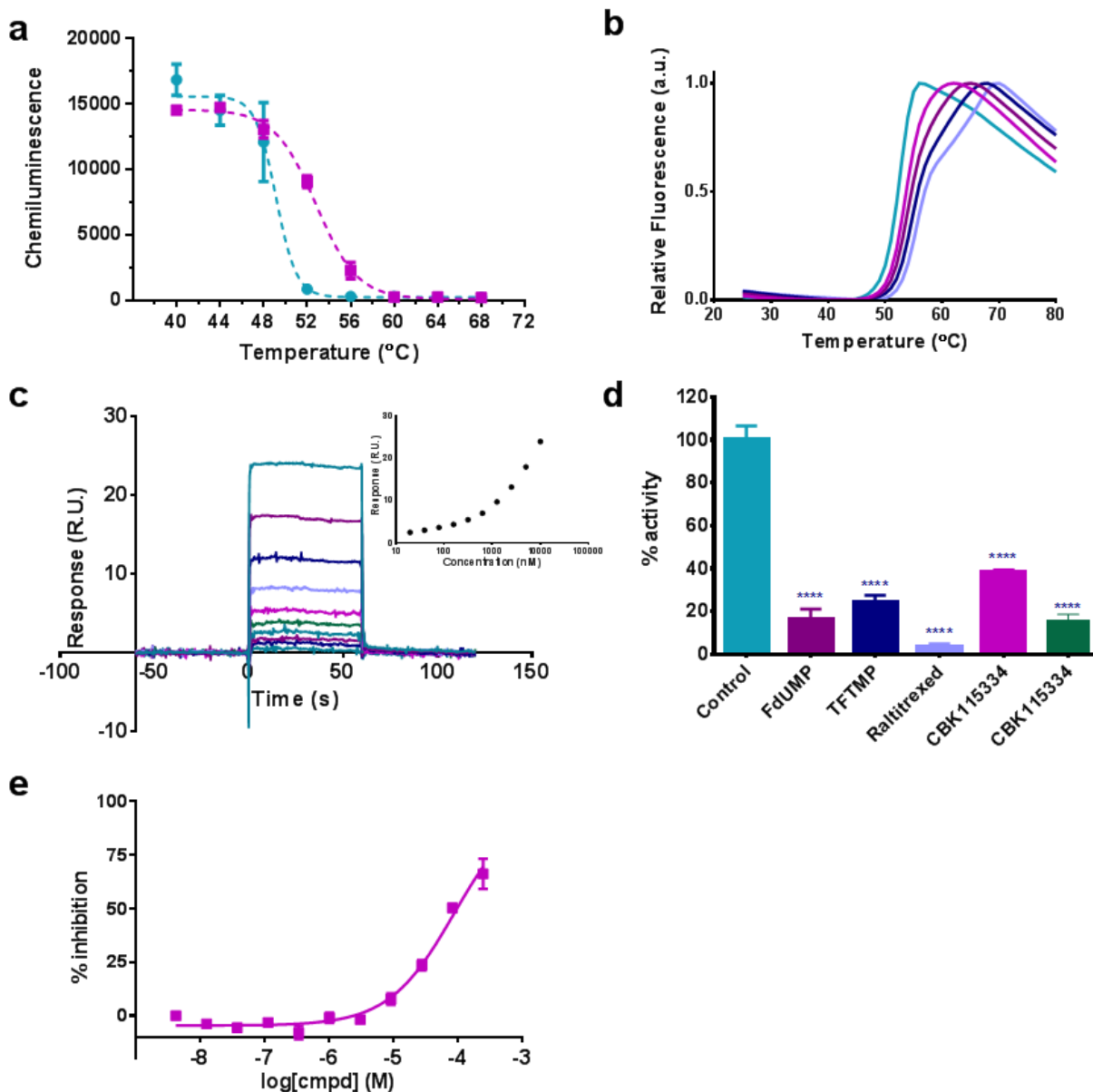
Instrument 1 6/30/2015 8:35:19 AM

Page 1 of 2

C



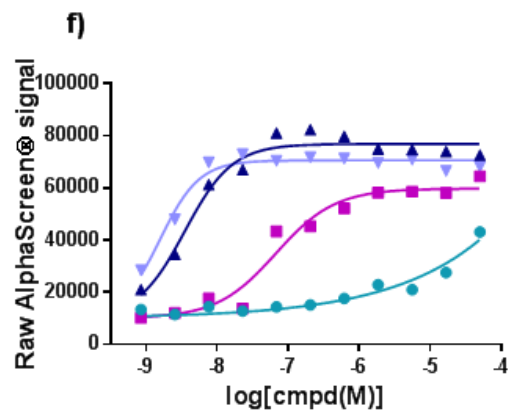
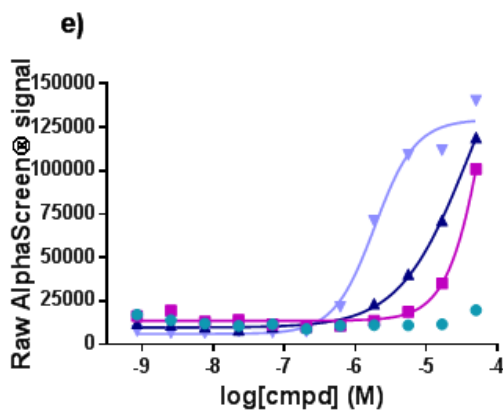
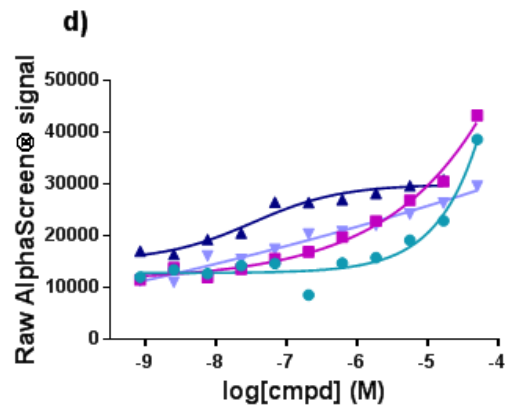
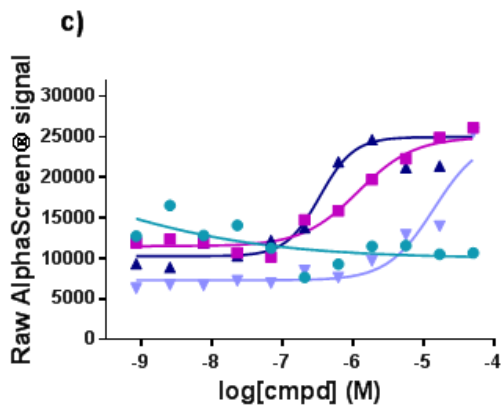
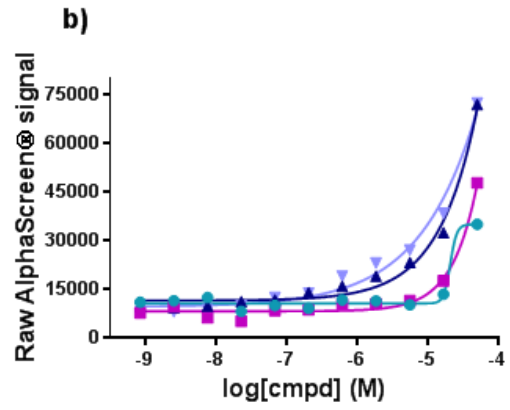
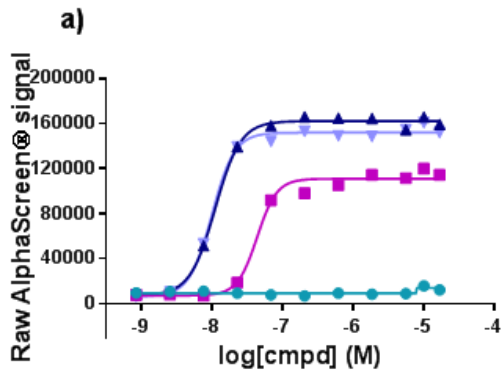
**Supplementary Figure 11| Characterization of the novel thymidylate synthase inhibitor CBK115334 using nuclear magnetic resonance (NMR) spectroscopy and high-pressure liquid chromatography (HPLC).** (a)  $^1\text{H}$  NMR spectra of CBK115334 in deuterated DMSO using a Bruker DPX400 spectrometer (400 MHz). Chemical shifts are as follows:  $^1\text{H}$  NMR (400 MHz,  $\text{DMSO}-d_6$ )  $\delta$  ppm 2.58 (d,  $J=0.95$  Hz, 3 H) 6.19 (s, 1 H) 7.48 - 7.59 (m, 3 H) 7.61 - 7.73 (m, 2 H) 7.98 (br. s., 2 H) 12.17 - 12.71 (s, 1 H).  $^1\text{H}$ -NMR confirmed the expected compound. (b) Results from HPLC-MS analysis on an Agilent/HP 1200 system 6110 mass spectrometer with electrospray ionization (ESI+). HPLC-MS methods were as follows. Method 1: Waters XBridge C18 3.5  $\mu\text{m}$  column (3.0 mm  $\times$  50 mm), 3.5 min gradient mobile phase [ $\text{CH}_3\text{CN}$ ] / [10 mM  $\text{NH}_4\text{HCO}_3/\text{H}_2\text{O}$ ]. (c) Method 2: ACE C8 3  $\mu\text{m}$  column (3.0 mm  $\times$  50 mm), mobile phase [0.1% TFA/ $\text{CH}_3\text{CN}$ ] / [0.1% TFA/ $\text{H}_2\text{O}$ ]. Absorbance was monitored at  $305 \pm 90$  and 254 nm. All solvents used were HPLC grade. HPLC-MS confirmed the correct molecular mass and showed a pure compound. The compound is commercially available and previously known from the literature<sup>3,4</sup>.

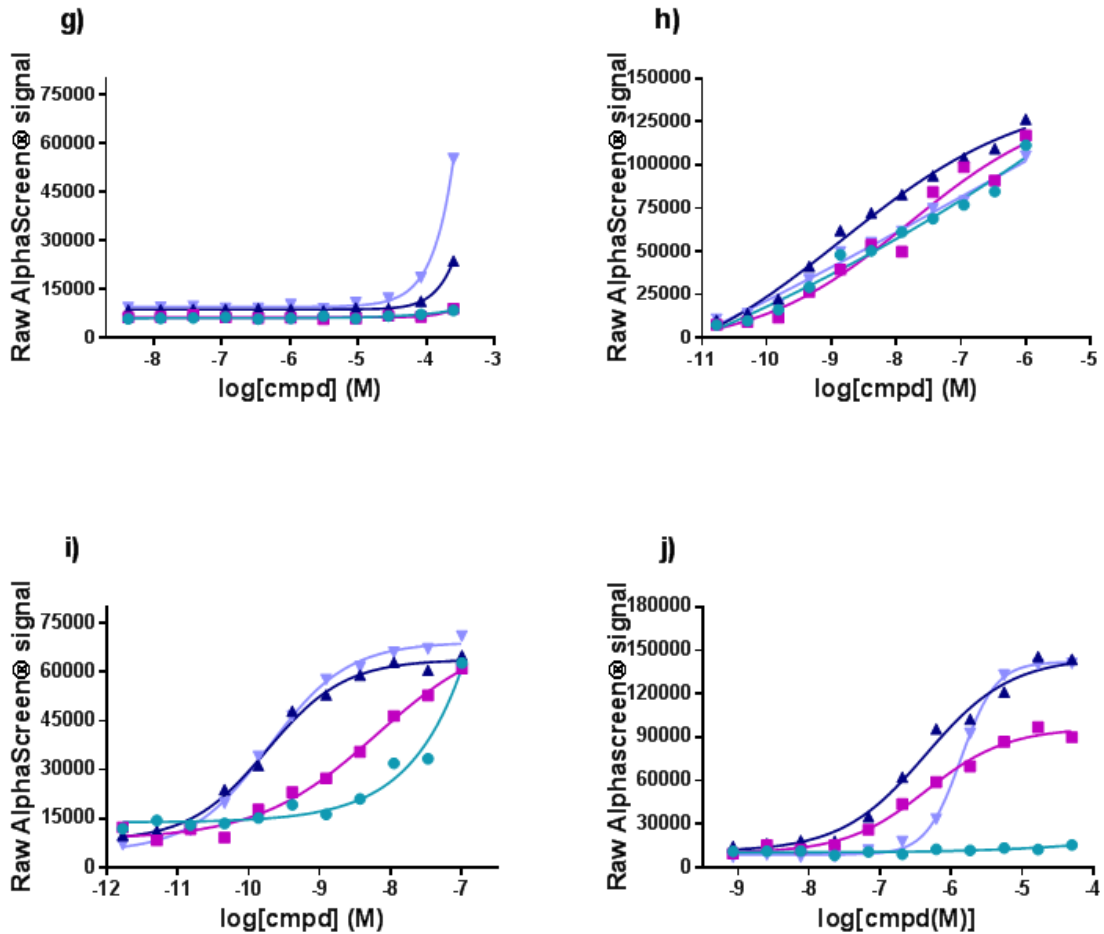


**Supplementary Figure 12| Thermal shift, surface plasmon resonance, in lysate CETSA and cell viability data for CBK115334.** (a) Western blot based CETSA derived  $T_{agg}$  curves for TS in K562 cell lysates in the presence of 200  $\mu$ M CBK115334 (magenta square) or DMSO (green circle). All experiments were performed on K562 cells using Western blots at a minimum of three independent replicates. (b) Thermal shift *in vitro* assay of CBK115334 in the presence of 500  $\mu$ M dUMP and DMSO (green), 12.5  $\mu$ M (magenta), 25  $\mu$ M (purple), 50  $\mu$ M (blue) and 100  $\mu$ M (lavender blue) CBK115334, respectively. (c) Sensorgrams and steady state affinity data from surface plasmon resonance experiments investigating the binding of CBK115334 to recombinant human thymidylate synthase in the presence of 200  $\mu$ M dUMP. The compound concentrations used were 10  $\mu$ M, 5  $\mu$ M, 2.5  $\mu$ M, 1.25  $\mu$ M, 625 nM, 312 nM, 156 nM, 78 nM, 39 nM and 20 nM (from top to bottom in the graph). The steady state data are shown in the insert. These data demonstrate binding to thymidylate synthase in the low  $\mu$ M range, but given that the signal does not saturate it is not possible to get an accurate estimate of the affinity. (d) TS activity in the presence of DMSO (green), 10  $\mu$ M

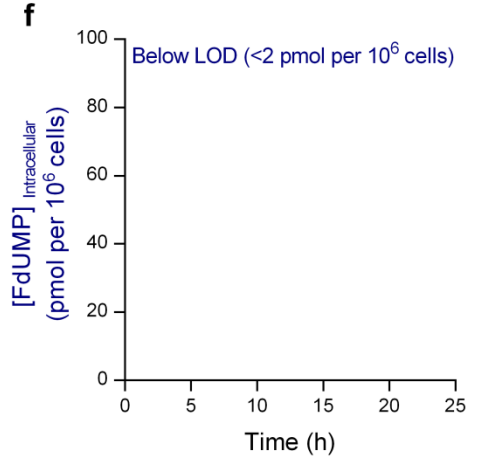
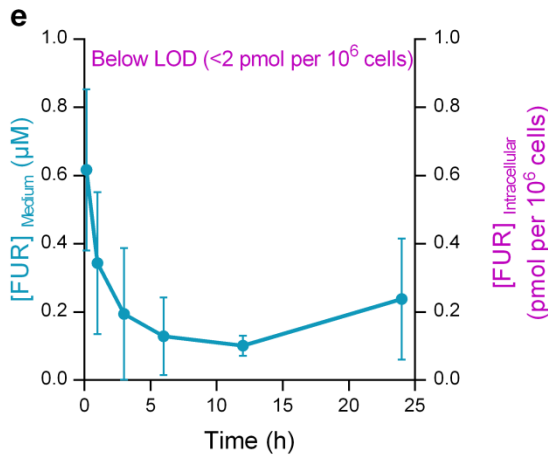
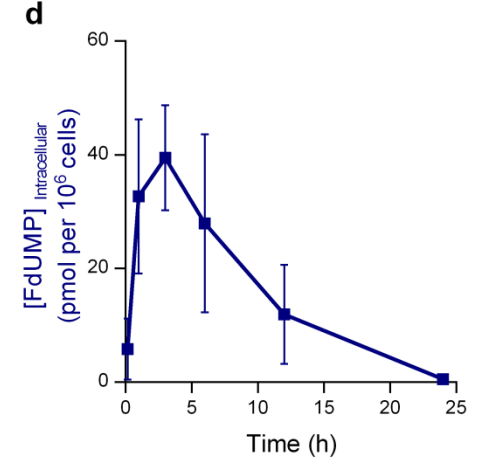
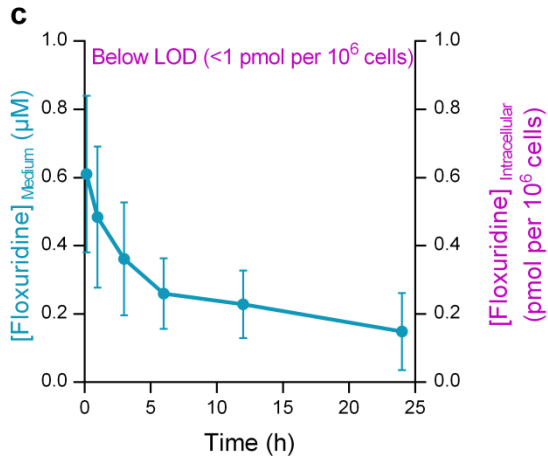
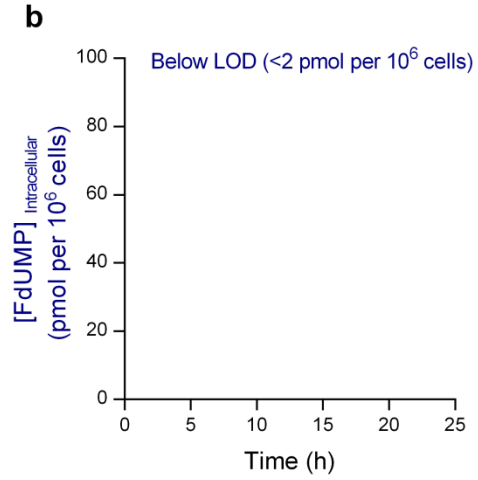
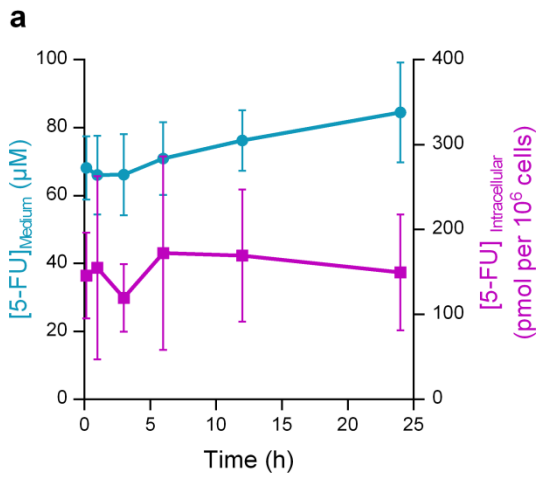
FdUMP (dark purple), 10  $\mu$ M TFTMP (blue), 10  $\mu$ M raltitrexed (lavender blue), 10  $\mu$ M CBK115334 (light purple) and 100  $\mu$ M CBK115334 (green), respectively. Data are presented as the average and S.E.M. of triplicate samples at one test occasion. (e) K562 cell viability measured following 72 hours incubation at 37°C and 5% CO<sub>2</sub> in the presence of different concentrations of CBK115334. All data were normalized based on DMSO and staurosporine controls to define complete inhibition. The solid line represents the best fit to a four-parameter dose-response model within GraphPad Prism resulting in a IC<sub>50</sub> value of 88±15  $\mu$ M. Data are presented as the average and S.E.M. of triplicate samples at one test occasion.

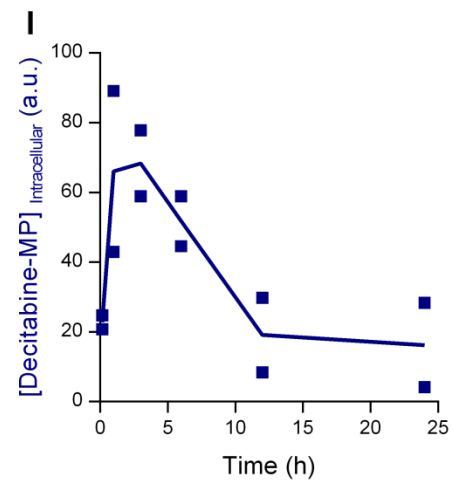
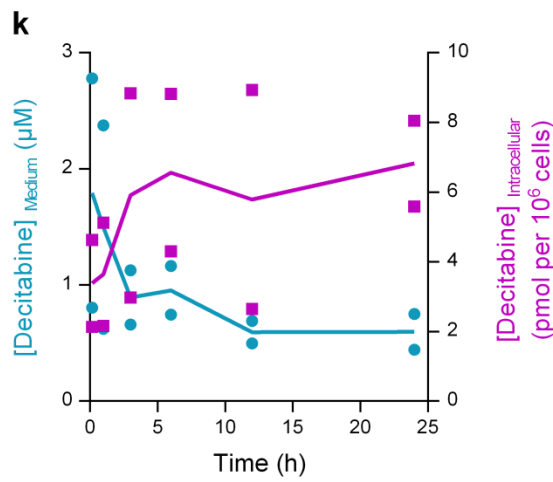
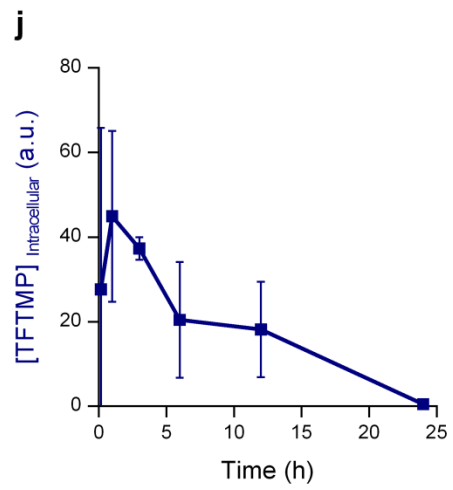
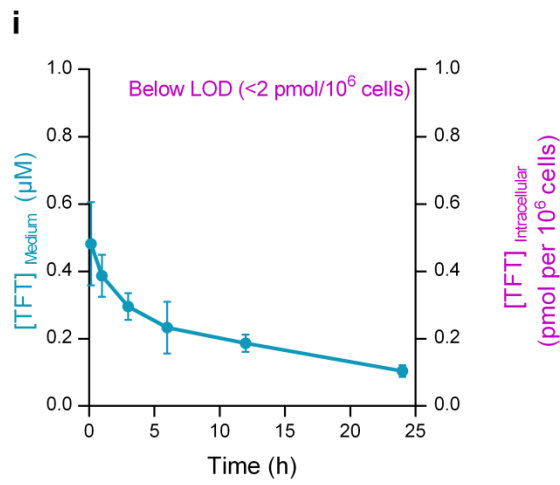
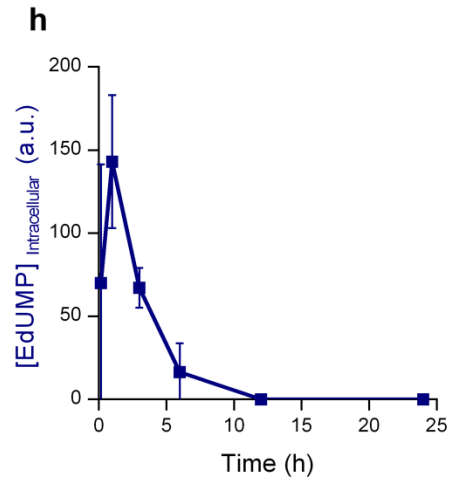
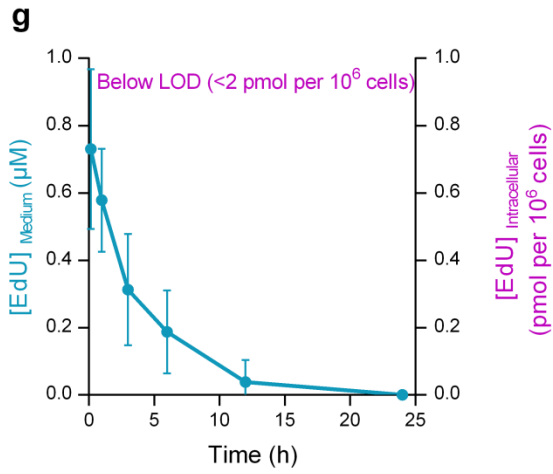


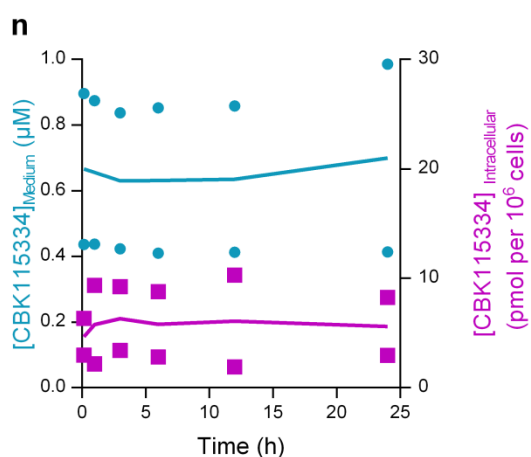
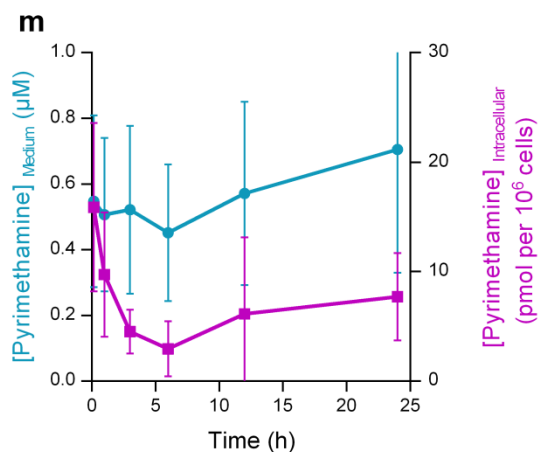




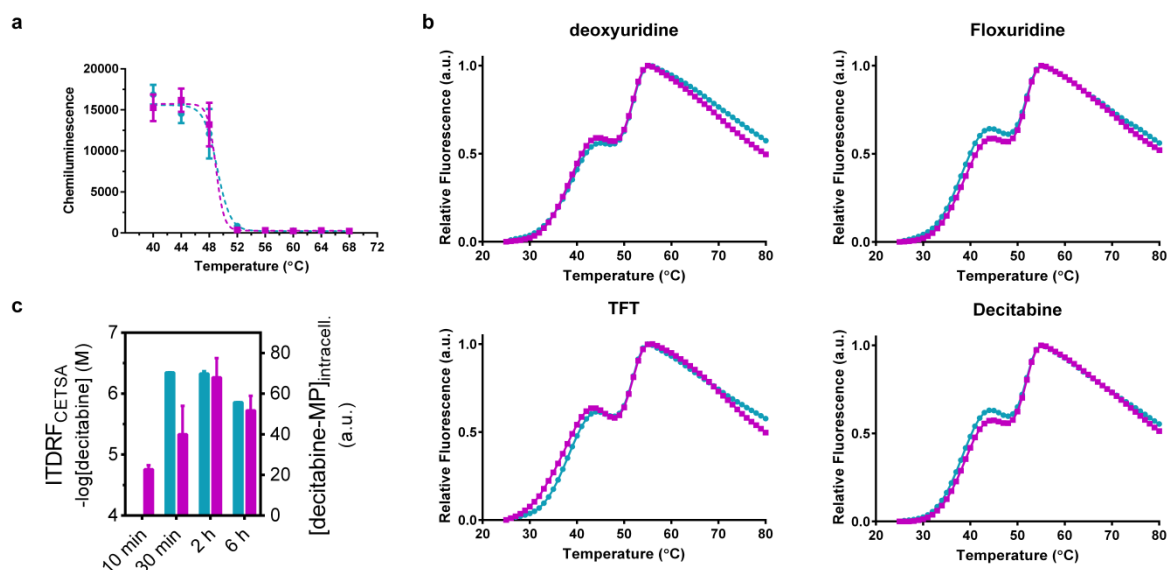
**Supplementary Figure 13| Isothermal dose-response fingerprints using CETSA for selected hit compounds as a function of pre-incubation time in K562 cells.** The ITDRF<sub>CETSA</sub> data were obtained by heating the cells transiently for 3 minutes at 50°C following various lengths of the pre-incubation time at a concentration of 5 million cells/ml. Symbols in each graph are as follows: 10 min (green circle), 30 min (magenta square), 2h (blue upwards triangle) and 6h (lavender blue downwards triangle). Data were obtained for methotrexate (a), CBK201253 (b), CBK201221 (c), CBK201230 (d), pyrimethamine (e), 5-fluorouridine (FUR), which was included in this effort although it was not part of the screen, (f), CBK115334 (g), 5-ethynyl-2'-deoxyuridine (EdU) (h), 5-trifluoro-2'-deoxythymidine (TFT) (i), and decitabine (j). The solid lines represent best fits to a saturation binding curve function resulting in half-maximal stabilization of thymidylate synthase. Representative data are provided as the average and S.E.M. from experiments done in quadruplicate at one test occasion. Some compounds were tested at two occasions as shown in Fig. 3 in the main text. Final concentrations of the assay reagents in the detection step was 1 nM rabbit polyclonal anti-TS IgG (15047-1-AP, Proteintech), 0.4 nM mouse monoclonal anti-TS IgG (sc-376161, Santa Cruz), 40  $\mu\text{g mL}^{-1}$  AlphaScreen® anti-mouse donor beads and 10  $\mu\text{g mL}^{-1}$  AlphaScreen® anti-rabbit acceptor beads.



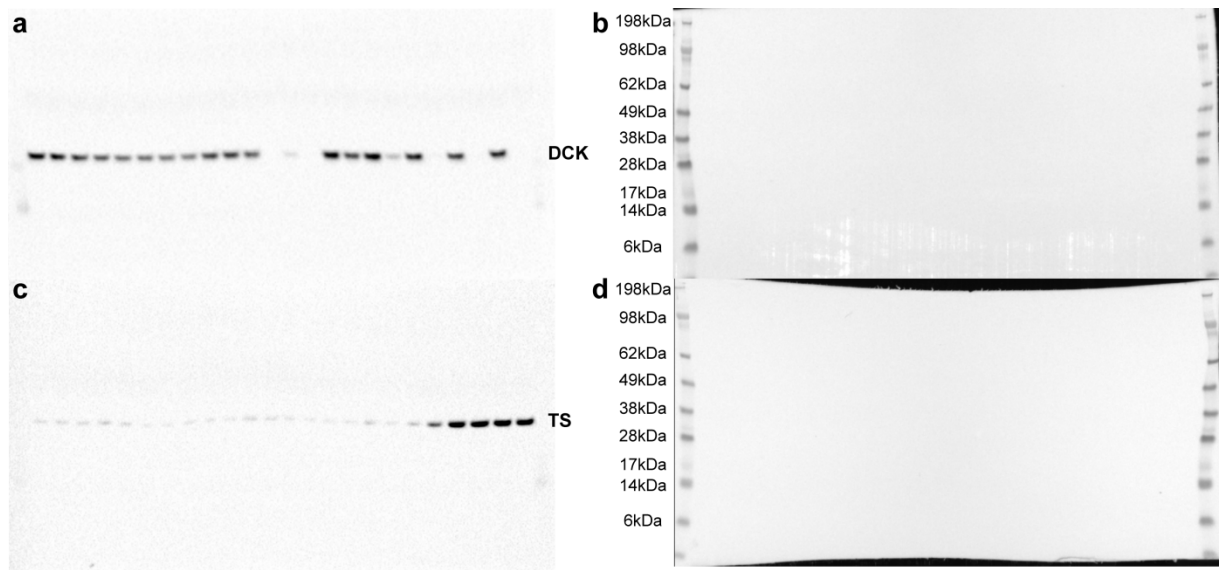




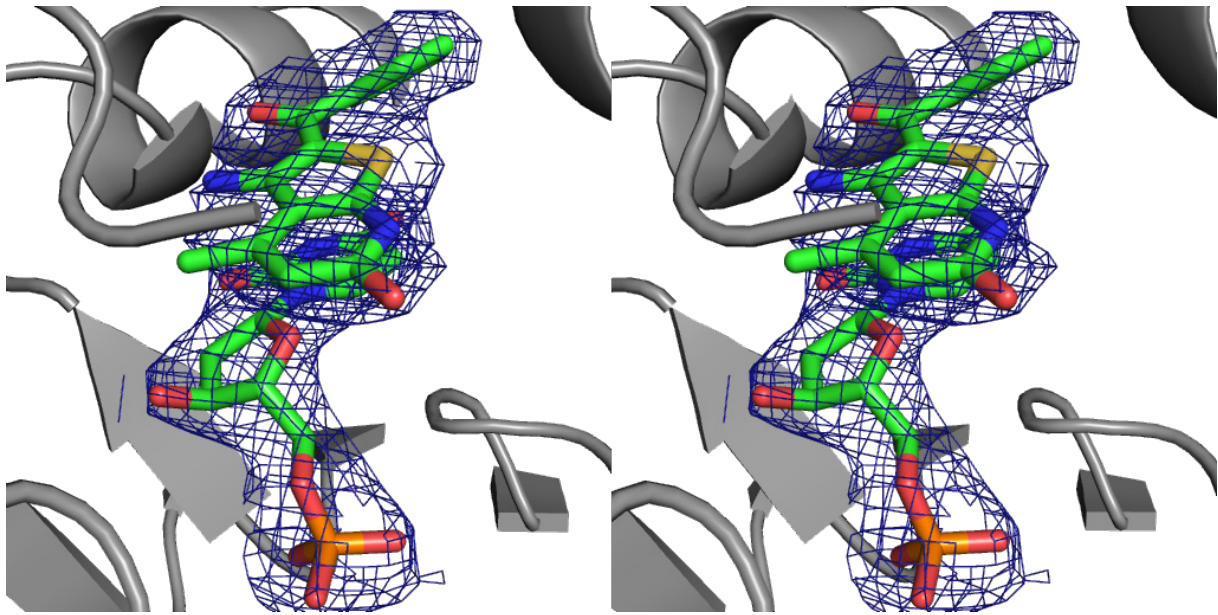
**Supplementary Figure 14| Data on extracellular and intracellular concentrations of selected hit compounds using LC-MS.** Extracellular (green circle) and intracellular concentrations of selected hit compounds (magenta square) and monophosphorylated metabolites (blue square) measured after various pre-incubation times with K562 cells using LC-MS/MS. **(a,b)** Incubation with 100 µM 5-FU. **(c,d)** Incubation with 1 µM floxuridine. **(e,f)** Incubation with 1 µM 5-fluorouridine (FUR) (included in this effort although it was not part of the screen). **(g,h)** Incubation with 1 µM EdU. **(i,j)** Incubation with 1 µM TFT. **(k,l)** Incubation with 1 µM decitabine. **(m)** Incubation with 1 µM pyrimethamine. **(n)** Incubation with 1 µM CBK115334.



**Supplementary Figure 15| Western blot based CETSA data on K562 lysates, thermal shift data on recombinant thymidylate synthase and time dependence of target engagement in K562 cells for decitabine. (a)**  $T_{agg}$  curves for TS in the presence of 200  $\mu$ M decitabine (magenta square) or DMSO (green circle). The experiment was performed on K562 cell lysates using Western blots at a minimum of three independent replicates. **(b)** Thermal shift *in vitro* assay for selected nucleosides (magenta) and controls (green). Apo-TS protein (control) has a bi-phasic melting profile. **(c)** Half-maximal stabilization of TS observed in CETSA experiments (green) and intracellular concentration of FdUMP (magenta) as a function of preincubation time with decitabine (see also Supplementary Figs. 13j and 14i for details). The CETSA data are presented as the average and range from two independent experiments. The LC-MS/MS data are provided as the average and S.E.M. from experiments done at three different occasions.



**Supplementary Figure 16| Full blots from CETSA experiments on decitabine metabolism.** (a) Chemiluminescence blot probing DCK levels (corresponding to Fig. 4b in main text) (b) The corresponding molecular weight marker image. (c) Chemiluminescence blot probing TS levels (corresponding to Fig. 4c in the main text). (d) The corresponding molecular weight marker image.



**Supplementary Figure 17| Stereo image of the electron density map for dUMP and CBK115334 in the active site of thymidylate synthase.** The 2Fo-Fc map around dUMP and CBK115334 is contoured in blue at 1.0 sigma level.



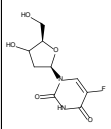
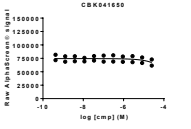
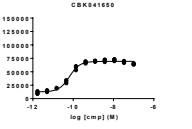
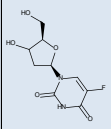
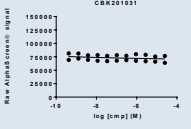
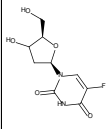
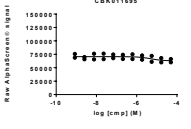
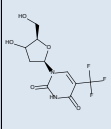
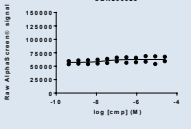
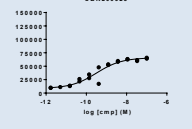
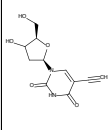
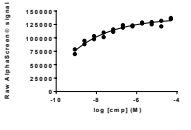
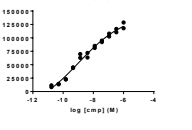
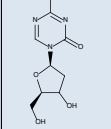
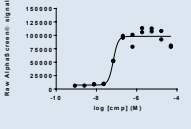
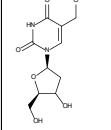
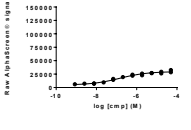
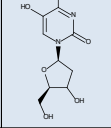
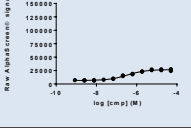
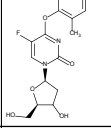
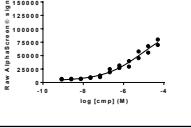
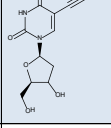
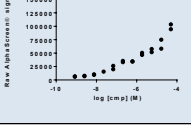
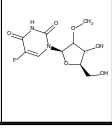
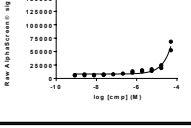
**Supplementary Table 1** | Rabbit and mouse derived antibodies directed towards human thymidylate synthase and tested in the AlphaScreen® assay

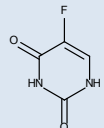
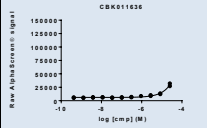
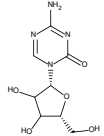
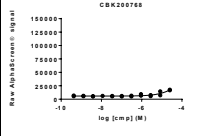
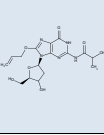
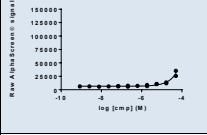
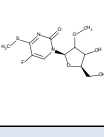
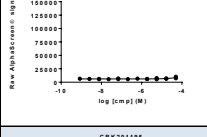
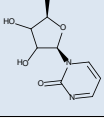
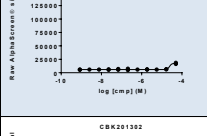
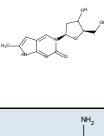
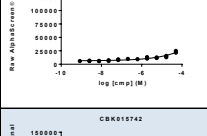
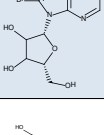
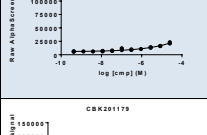
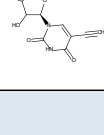
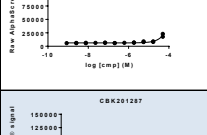
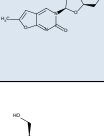
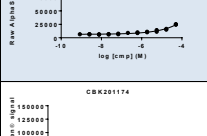
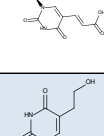
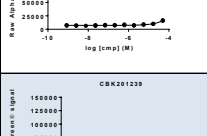
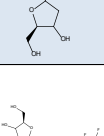
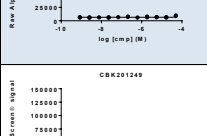
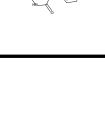
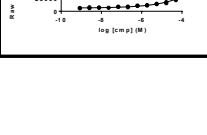
| Antibody  | Species | Isotype       | Vendor         | Product number | Recognized epitope                                 | Vendor claimed validity for:         |
|-----------|---------|---------------|----------------|----------------|--|--------------------------------------|
| <b>M1</b> | Mouse   | IgG1          | Santa Cruz     | sc-33679       | Recombinant TS                                     | WB, IP, IF, IHC(P) and FCM           |
| <b>M2</b> | Mouse   | IgG1          | Santa Cruz     | sc-56492       | Recombinant TS                                     | WB, IP, IF and FCM                   |
| <b>M3</b> | Mouse   | IgG2b         | Santa Cruz     | sc-376161      | Amino acids 99-127 within an internal region of TS | WB, IP, IF, IHC(P) and ELISA         |
| <b>M4</b> | Mouse   | IgG1 $\kappa$ | Sigma Aldrich  | WH0007298M1    | Amino acids 111-211                                | IHC, indirect ELISA, indirect IF, WB |
| <b>R1</b> | Rat     |               | Avivasysbio    | ARP48543_P050  | C-terminal region                                  | WB                                   |
| <b>R2</b> | Rat     | IgG           | Proteintech    | 15047-1-AP     | Recombinant TS                                     | ELISA, WB, IHC, IF                   |
| <b>R3</b> | Rat     | IgG           | Cell signaling | D5B3           | Residues near the C-terminus                       | WB, IF, IHC and FC                   |

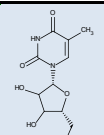
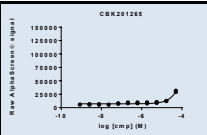
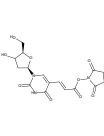
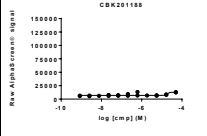
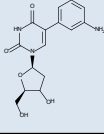
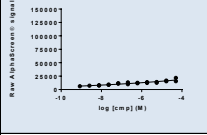
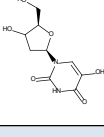
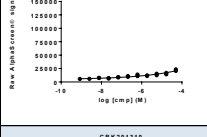
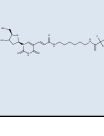
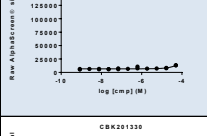
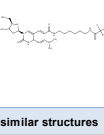
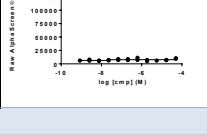
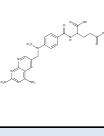
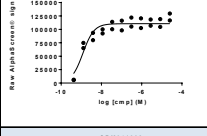
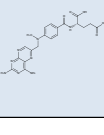
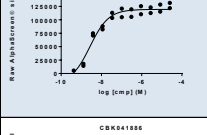
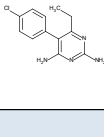
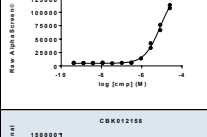
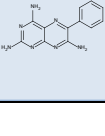
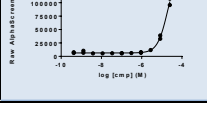
**Supplementary Table 2** | Small molecule screening information

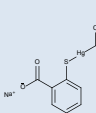
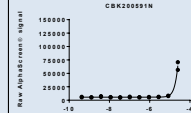
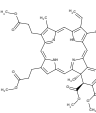
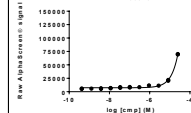
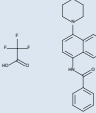
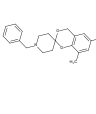
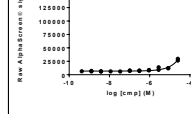
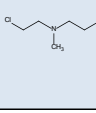
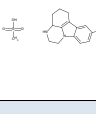
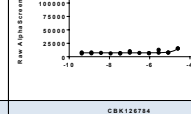
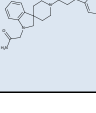
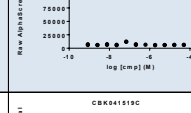
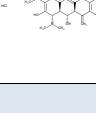
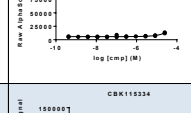
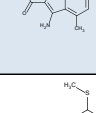
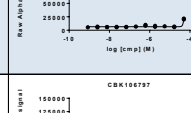
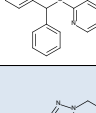
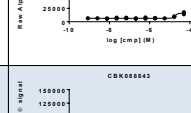
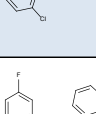
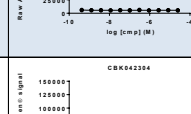
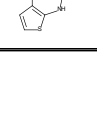
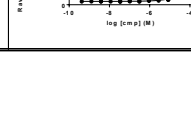
| Category                                 | Parameter                           | Description   |
|--|-------------------------------------|---|
| <b>Assay</b>                             | Type of assay                       | CETSA, Cellular Thermal Shift Assay with AlphaScreen® detection of target protein   |
|  | Target                              | Human thymidylate synthase; TS; dTMP synthase   |
|  | Primary measurement                 | Detection of remaining native TS after heat challenge in presence of test compounds.  |
|  | Key reagents                        | Anti-rabbit IgG (Fc specific) AlphaLISA® Acceptor Beads, PerkinElmer, AL104C<br>Anti-Mouse IgG Alpha Donor beads, PerkinElmer, AS104D<br>Anti TS mouse monoclonal IgG2b, Santa Cruz Biotechnology, sc-376161<br>Anti TS rabbit polyclonal, Proteintech, 15047-1-AP<br>AlphaLISA Immunoassay buffer 10X, PerkinElmer, AL000C<br>Surefire lysis buffer 5X, Perkin Elmer                                   |
|  | Assay protocol                      | See online methods and supplementary results.   |
|  | Additional comments                 |   |
| <b>Library</b>                           | Library size                        | 10,928 compounds  |
|  | Library composition                 | The library consists of a chemically diverse collection of compounds containing both commercial and internal compounds (donation from Biovitrum). The tested compounds includes also 1199 known bioactive molecules from the Prestwick chemical library and 192 nucleosides from Barry and Associates   |
|  | Source                              | The screen was done based on plating of 10 mM DMSO solutions from Labcyte 384 LDV plates using an Echo 550  |
|  | Additional comments                 | See Online Materials for further details on the composition of the CBCS primary screening set   |
| <b>Screen</b>                            | Format                              | 384-well format.<br>Compound plate: 384-well PP plate, Greiner, 784201<br>Assay plate: 384-well PCR plates from Bio-Rad, HSR-4805<br>Detection plate: 384-well Optiplate, Perkin Elmer, 6008280   |
|  | Concentration(s) tested             | Compound concentration 50 µM, DMSO concentration 0.5%   |
|  | Plate controls                      | Positive control 100 nM Raltitrexed<br>Negative control 0.5% DMSO   |
|  | Reagent/ compound dispensing system | Compound dispensing system: Echo 550 from Labcyte<br>Reagent dispensing system: Multidrop combi from Thermo Scientific, FlexDrop IV from PerkinElmer and Bravo Automated Liquid Handling Platform from Agilent  |
|  | Detection instrument and software   | Plate heating: Lightcycler 480 from Roche<br>Detection: Envision 2104 multilabel reader from PerkinElmer  |
|  | Assay validation/QC                 | Positive control: average 9308, standard deviation 932<br>Negative control: average 148051, standard deviation 28860<br>Average Z' factor/plate: 0.83   |
|  | Correction factors                  | Not applicable  |
|  | Normalization                       | Data are normalized to the positive (100% stabilization) and negative controls (0% stabilization) on each plate and are expressed as % stabilization  |
|  | Additional comments                 | The screen was done at Chemical Biology Consortium Sweden at Karolinska institutet, Sweden  |
|  | <b>Post-HTS analysis</b>            | Hit criteria  |
| Hit rate                                 |                                     | 0.6%  |
| Additional assay(s)                      |                                     | Retesting of hits in CETSA screening assay at 11 concentrations. Retesting of a selection of hits in screening assay at 11 concentrations as a function of incubation time. Selected hits tested using Western blot based CETSA protocol. Measurements of intracellular concentrations for selected hits. Selected compound verified using Tm shifts, surface plasmon resonance and co-crystallization. |
| Confirmation of hit purity and structure |                                     | ID and purity analysis with LC-UV/MS detection  |
|  | Additional comments                 |   |

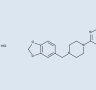
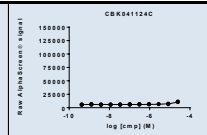
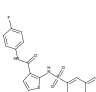
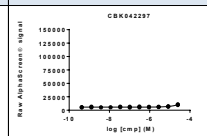
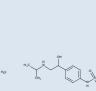
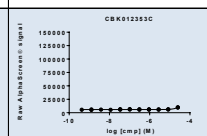
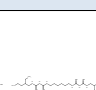
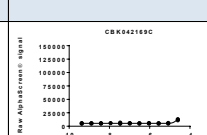
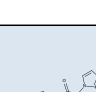
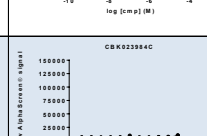

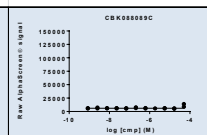
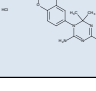
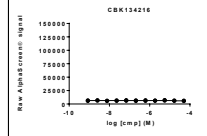
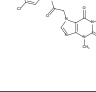
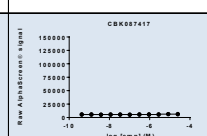
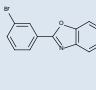
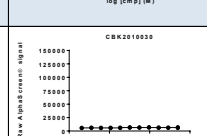
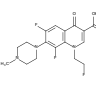
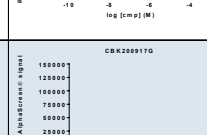
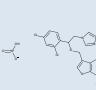
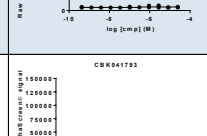
**Supplementary Table 3** | Summary data for identified hits in the CETSA-HTS on thymidylate synthase

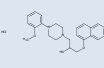
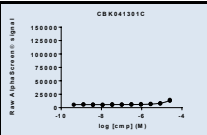
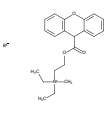
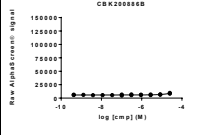
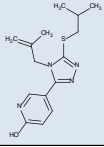
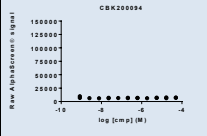
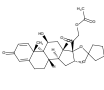
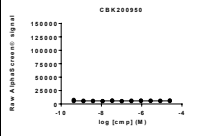
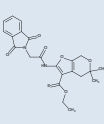
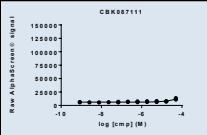
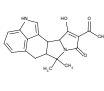
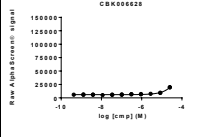
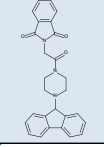
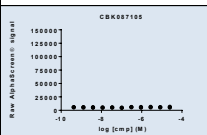
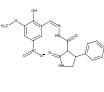
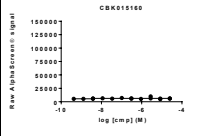
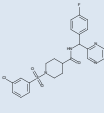
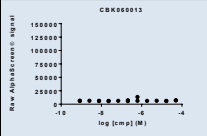
| Compound ID | Structure   | Listed drug in THOMSON REUTERS Integrity | Name                                | % stabilization in screen | Hit confirmation ITRF <sub>CETSA</sub>  | New dilutions ITRF <sub>CETSA</sub>  | ITRF <sub>CETSA</sub> | Expected mass found | % Purity |     |
|-------------|---|--|-------------------------------------|---------------------------|---|--|-----------------------|---------------------|----------|-----|
| CBK041650   |    | Yes                                      | Floxuridine<br>5-fluorodeoxyuridine | 64                        |    |    | 6.61E-11              | YES                 | N.D.     |     |
| CBK201031   |    | Yes                                      | Floxuridine<br>5-fluorodeoxyuridine | 66                        |    |  |                       | N.D.                | N.D.     |     |
| CBK011695   |    | Yes                                      | Floxuridine<br>5-fluorodeoxyuridine | 56                        |    |  |                       | YES                 | 100      |     |
| CBK200925   |    | Yes                                      | Trifluridine<br>Trifluorothymidine  | 66                        |    |    | 3.18E-10              | N.D.                | N.D.     |     |
| CBK201207   |  |  |                                     | 102                       |  |  | 1.41E-09              | YES                 | 100      |     |
| CBK201329   |  | Yes                                      | Dectabine<br>5-Aza-deoxycytidine    | 91                        |  |  |                       | YES                 | 100      |     |
| CBK201230   |  |  |                                     | 23                        |  |  |                       | 1.42E-07            | YES      | 66  |
| CBK201221   |  |  |                                     | 22                        |  |  |                       | 3.43E-07            | YES      | 100 |
| CBK201184   |  |  |                                     | 66                        |  |  |                       | 9.17E-06            | YES      | 100 |
| CBK201182   |  |  |                                     | 90                        |  |  |                       | 2.28E-05            | YES      | 100 |
| CBK201253   |  |  |                                     | 61                        |  |  |                       | N.D.                | YES      | 100 |

|           |   |     |                                |    |   |  |      |      |      |
|-----------|---|-----|--------------------------------|----|---|--|------|------|------|
| CBK011636 |    | Yes | 5-Fluorouracil<br>Fluorouracil | 48 |    |  | N.D. | N.D. | N.D. |
| CBK200768 |    | Yes | Azacitidine<br>5-Azacytidine   | 32 |    |  | N.D. | YES  | 100  |
| CBK201216 |    |     |                                | 30 |    |  | N.D. | YES  | 100  |
| CBK201267 |    |     |                                | 23 |    |  | N.D. | YES  | 100  |
| CBK201195 |    |     |                                | 22 |    |  | N.D. | YES  | 100  |
| CBK201302 |   |     |                                | 21 |   |  | N.D. | YES  | 100  |
| CBK015742 |  |     |                                | 20 |  |  | N.D. | YES  | 100  |
| CBK201179 |  |     |                                | 20 |  |  | N.D. | YES  | 100  |
| CBK201287 |  |     |                                | 20 |  |  | N.D. | YES  | 100  |
| CBK201174 |  |     |                                | 17 |  |  | N.D. | YES  | 100  |
| CBK201239 |  |     |                                | 17 |  |  | N.D. | YES  | 100  |
| CBK201249 |  |     |                                | 17 |  |  | N.D. | YES  | 99   |

|  |   |     |               |    |   |  |          |     |     |
|--|---|-----|---------------|----|---|--|----------|-----|-----|
| CBK201265                                  |    |     |               | 17 |    |  | N.D.     | YES | 100 |
| CBK201188                                  |    |     |               | 16 |    |  | N.D.     | YES | 92  |
| CBK201262                                  |    |     |               | 16 |    |  | N.D.     | NO  | 100 |
| CBK201317                                  |    |     |               | 16 |    |  | N.D.     | YES | 100 |
| CBK201310                                  |    |     |               | 15 |    |  | N.D.     | YES | 93  |
| CBK201330                                  |   |     |               | 13 |   |  | N.D.     | YES | 95  |
| <b>Anti-folates and similar structures</b> |   |     |               |    |   |  |          |     |     |
| CBK200695                                  |  | Yes | Amethopterin  | 94 |  |  | 9.42E-10 | YES | 90  |
| CBK041938                                  |  | Yes | Methotrexate  | 96 |  |  | 2.70E-09 | YES | 98  |
| CBK041886                                  |  | Yes | Pyrimethamine | 76 |  |  | 8.38E-06 | YES | 99  |
| CBK012158                                  |  | Yes | Triamterene   | 78 |  |  | N.D.     | YES | 99  |

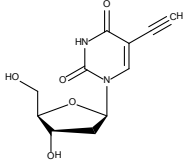
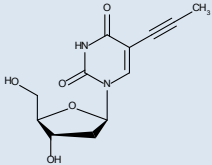
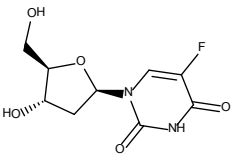
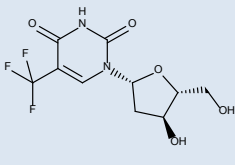
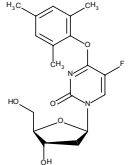
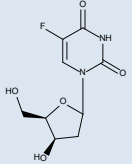
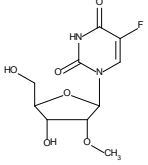
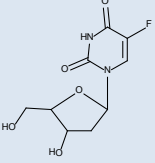
| Other      |   |     |                          |     |   |  |      |      |      |
|------------|---|-----|--------------------------|-----|---|--|------|------|------|
| CBK200591N |    | Yes | Thimerosal<br>Thiomersal | 115 |    |  | N.D. | YES  | 100  |
| CBK200926  |    |     |                          | 81  |    |  | N.D. | YES  | 99   |
| CBK028412T |    |     |                          | 64  | Out of stock  |  | N.D. | N.D. | N.D. |
| CBK061572  |    |     |                          | 28  |    |  | N.D. | YES  | 100  |
| CBK041969  |    | Yes |                          | 24  | Out of stock  |  | N.D. | N.D. | N.D. |
| CBK200931G |  | Yes | Pirlindole<br>Pyrazidol  | 23  |  |  | N.D. | YES  | 99   |
| CBK126784  |  |     |                          | 22  |  |  | N.D. | YES  | 96   |
| CBK041519C |  |     |                          | 20  |  |  | N.D. | NO   | N.D. |
| CBK115334  |  |     |                          | 20  |  |  | N.D. | YES  | 100  |
| CBK106797  |  |     |                          | 19  |  |  | N.D. | YES  | 80   |
| CBK088843  |  |     |                          | 18  |  |  | N.D. | YES  | 100  |
| CBK042304  |  |     |                          | 17  |  |  | N.D. | YES  | 90   |

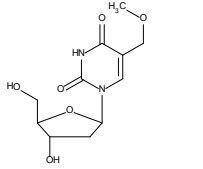
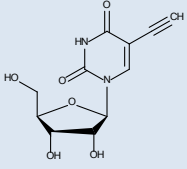
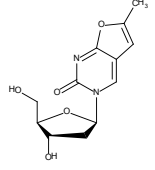
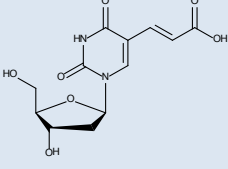
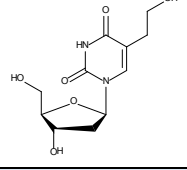
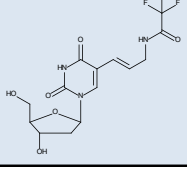
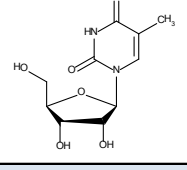
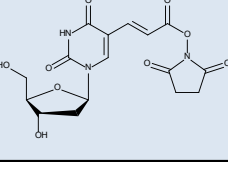
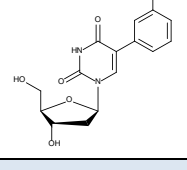
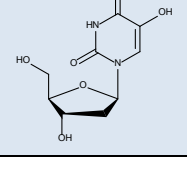
|                                     |   |     |                       |    |   |  |      |     |     |  |
|-------------------------------------|---|-----|-----------------------|----|---|--|------|-----|-----|--|
| CBK041124C                          |    | Yes | Piribedil             | 17 |    |  | N.D. | NO  | 100 |  |
| CBK042297                           |    |     |                       | 16 |    |  | N.D. | YES | 95  |  |
| CBK012353C                          |    | Yes | Sotalol               | 14 |    |  | N.D. | YES | 100 |  |
| CBK042169C                          |    |     |                       | 14 |    |  | N.D. | YES | 95  |  |
| CBK023984C                          |    |     |                       | 13 |    |  | N.D. | YES | 100 |  |
| <b>Inactive in hit confirmation</b> |   |     |                       |    |   |  |      |     |     |  |
| CBK088089C                          |    |     |                       | 63 |   |  | N.D. | YES | 98  |  |
| CBK134216                           |  |     |                       | 50 |  |  | N.D. | YES | 100 |  |
| CBK087417                           |  |     |                       | 76 |  |  | N.D. | YES | 92  |  |
| CBK201030                           |  | Yes | Fleroxacin            | 66 |  |  | N.D. | YES | 100 |  |
| CBK200917G                          |  | Yes | Sertaconazole nitrate | 66 |  |  | N.D. | YES | 100 |  |
| CBK041793                           |  | Yes | Celecoxib             | 61 |  |  | N.D. | YES | 100 |  |

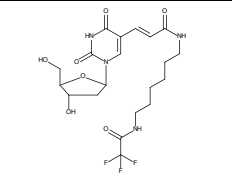
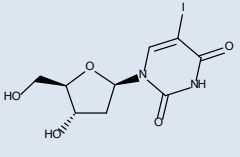
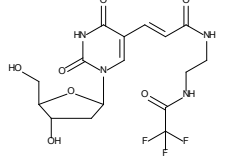
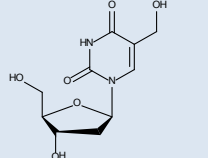
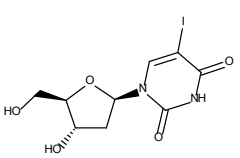
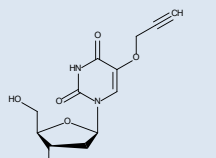
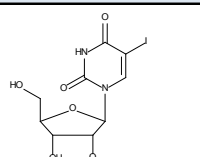
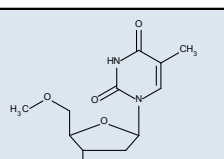
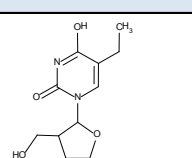
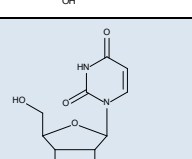
|            |   |     |  |    |   |  |      |     |     |
|------------|---|-----|--|----|---|--|------|-----|-----|
| CBK041301C |    | Yes | Naftopidil   | 59 |    |  | N.D. | YES | 99  |
| CBK200886B |    |     |  | 58 |    |  | N.D. | YES | 95  |
| CBK200094  |    |     |  | 58 |    |  | N.D. | YES | 100 |
| CBK200950  |    | Yes | Amcinonid<br>Amciderm<br>Cyclocort<br>Pentocort<br>Visderm | 56 |    |  | N.D. | YES | 100 |
| CBK087111  |    |     |  | 55 |    |  | N.D. | YES | 95  |
| CBK006628  |   |     |  | 55 |   |  | N.D. | YES | 84  |
| CBK087105  |  |     |  | 52 |  |  | N.D. | YES | 93  |
| CBK015160  |  |     |  | 52 |  |  | N.D. | YES | 93  |
| CBK060013  |  |     |  | 34 |  |  | N.D. | YES | 87  |



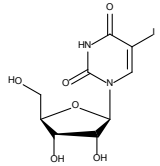
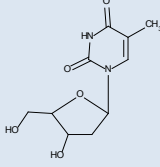
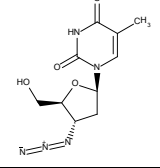
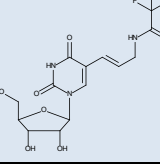
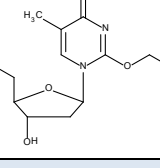
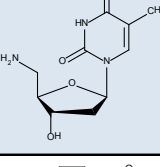
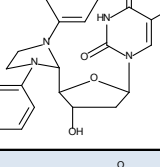
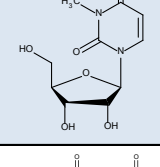
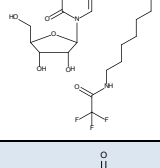
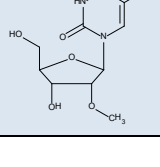
**Supplementary Table 4** | Shortlist of compounds that were investigated as potential actives based on structural resemblance to known thymidylate synthase inhibitors

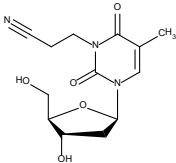
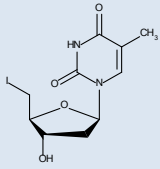
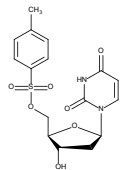
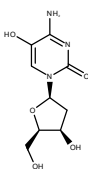
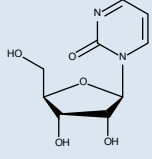
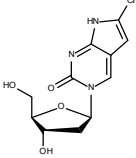
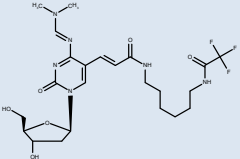
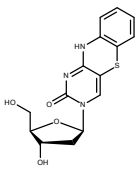
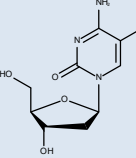
| Compound ID                   | Structure   | % stabilization in screen |
|-------------------------------|---|---------------------------|
| <b>Uracil-based analogues</b> |   |                           |
| CBK201207                     |    | 102                       |
| CBK201182                     |    | 90                        |
| CBK201031                     |    | 66                        |
| CBK200925                     |  | 66                        |
| CBK201184                     |  | 66                        |
| CBK041650                     |  | 64                        |
| CBK201253                     |  | 61                        |
| CBK011695                     |  | 56                        |

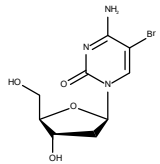
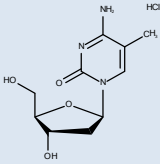
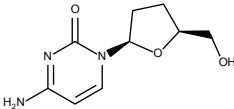
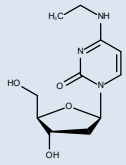
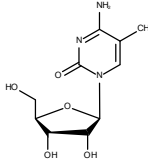
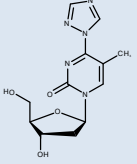
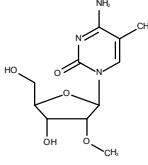
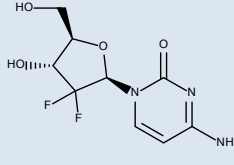
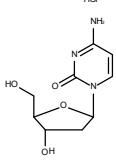
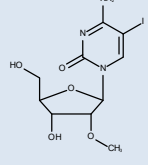
|           |   |    |
|-----------|---|----|
| CBK201230 |    | 23 |
| CBK201179 |    | 20 |
| CBK201287 |    | 20 |
| CBK201174 |    | 17 |
| CBK201239 |   | 17 |
| CBK201249 |  | 17 |
| CBK201265 |  | 17 |
| CBK201188 |  | 16 |
| CBK201262 |  | 16 |
| CBK201317 |  | 16 |

|           |   |    |
|-----------|---|----|
| CBK201310 |    | 15 |
| CBK200650 |    | 10 |
| CBK201214 |    | 9  |
| CBK201332 |    | 9  |
| CBK200650 |   | 8  |
| CBK201278 |  | 7  |
| CBK201211 |  | 5  |
| CBK201338 |  | 4  |
| CBK041677 |  | 3  |
| CBK201166 |  | 1  |

|           |  |    |
|-----------|--|----|
| CBK087642 |  | 0  |
| CBK201159 |  | 0  |
| CBK201200 |  | 0  |
| CBK201279 |  | 0  |
| CBK201256 |  | 0  |
| CBK201280 |  | 0  |
| CBK201180 |  | -1 |
| CBK201339 |  | -1 |
| CBK201270 |  | -1 |
| CBK201316 |  | -1 |

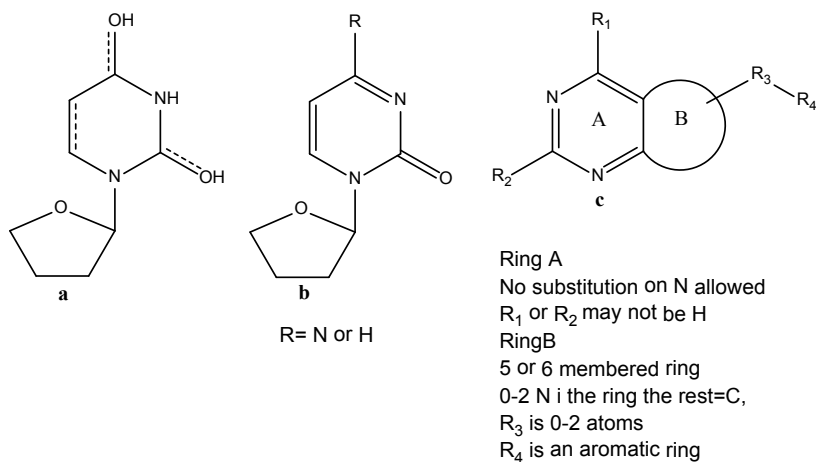
|           |   |    |
|-----------|---|----|
| CBK201304 |    | -1 |
| CBK011998 |    | -1 |
| CBK041618 |    | -1 |
| CBK201298 |    | -1 |
| CBK201334 |   | -1 |
| CBK201315 |  | -1 |
| CBK201232 |  | -1 |
| CBK201281 |  | -1 |
| CBK201231 |  | -1 |
| CBK201251 |  | -1 |

|                                 |   |    |
|---------------------------------|---|----|
| CBK201322                       |    | -1 |
| CBK201197                       |    | -1 |
| CBK201283                       |    | -2 |
| <b>Cytosine-based analogues</b> |   |    |
| CBK201221                       |    | 22 |
| CBK201195                       |  | 22 |
| CBK201302                       |  | 21 |
| CBK201330                       |  | 13 |
| CBK201237                       |  | 9  |
| CBK201226                       |  | 7  |

|           |   |   |
|-----------|---|---|
| CBK201161 |    | 5 |
| CBK201307 |    | 4 |
| CBK200928 |    | 0 |
| CBK201311 |    | 0 |
| CBK201268 |   | 0 |
| CBK201235 |  | 0 |
| CBK201227 |  | 0 |
| CBK200978 |  | 0 |
| CBK201203 |  | 0 |
| CBK201296 |  | 0 |

|           |  |    |
|-----------|--|----|
| CBK201274 |  | -1 |
| CBK201219 |  | -1 |
| CBK042058 |  | -1 |
| CBK200603 |  | -1 |
| CBK024684 |  | -1 |
| CBK201306 |  | -1 |

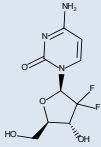
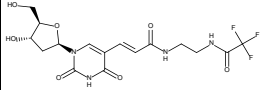
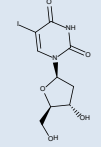
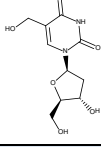
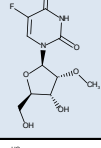
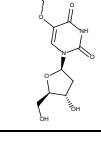
These compounds were identified based on sub-structure searches within the primary screening set of 10,928 compounds. These searches were based on uridine, cytidine and anti-folate like compounds according to the following rules:





The pyrimidine rings in **(a)** and **(b)** were allowed to vary in regards to any substitutions on the furan ring and on the base and included also variations of the bond character, *i.e.* single/double bonds as indicated in the structures. The general minimal structure element for anti-folate like structures **(c)** was determined based on a series of known inhibitors that has been tested in man as drugs or putative drugs targeting thymidylate synthase. Based on these criteria the searches resulted in 51 uracil-based analogs, 22 cytosine-based analogs and no anti-folate like structures in the screening library.

**Supplementary Table 5** | Additional data for compounds that were investigated as potential false negatives based on structural resemblance to known thymidylate synthase inhibitors

| Compound ID | Structure   | % stabilization at screen (2h preincubation) | % stabilization at retest (6h preincubation) |
|-------------|---|--|--|
| CBK200978   |    | 0  | 3  |
| CBK201214   |    | 9  | 6  |
| CBK200650   |    | 10   | 14   |
| CBK201332   |   | 9  | 7  |
| CBK201168   |  | 2  | 5  |
| CBK201278   |  | 7  | 12   |

To establish whether there were any obvious false negatives missed in the screen we used substructure searches based on clinically used TS inhibitors (see Methods for details and **Supplementary Table 4** for the outcome). Manual curation revealed the presence of these six compounds that motivated further experimental examination, including the cytidine analog gemcitabine, which was recently shown to weakly bind TS following phosphorylation and deamination to the corresponding uridine analog<sup>5</sup>. None of these resulted in significant target engagement using the present assay setup, even after prolonged pre-incubation times, thus confirming the original screen data. Apart from gemcitabine, these compounds are not previously reported as TS inhibitors showing that the CETSA-HTS approach selected accurately for known inhibitors with a low rate of false negatives.

**Supplementary Table 6** | Historical screening data for CBK115334

| Target source                | Assay type | Detection type | Concentration (M) | Inhibition (%) | Activation (%) | Hit |
|------------------------------|------------|----------------|-------------------|----------------|----------------|-----|
| Embryonic stem cells         | Cell-based | Luminescence   | 1,0E-05           |                | -12,5          | No  |
| Enzyme membrane preparation  | Enzymatic  | Absorbance     | 1,0E-05           | 12,2           |                | No  |
| Recombinant enzyme           | Enzymatic  | Absorbance     | 1,0E-05           | 25,6           |                | No  |
| Recombinant enzyme           | Enzymatic  | Absorbance     | 1,0E-05           | 18,3           |                | No  |
| Recombinant enzyme           | Enzymatic  | Absorbance     | 1,0E-05           | 12,7           |                | No  |
| Recombinant enzyme           | Enzymatic  | Absorbance     | 1,0E-05           | 2,3            |                | No  |
| Recombinant enzyme           | Enzymatic  | Absorbance     | 1,0E-05           | -3,9           |                | No  |
| Recombinant enzyme           | Enzymatic  | Absorbance     | 1,0E-05           | -2,5           |                | No  |
| Mammalian cell-line          | Cell-based | Imaging        | 1,3E-05           | -28,3          |                | No  |
| Mammalian cell-line          | Cell-based | Luminescence   | 1,0E-05           |                | 27,2           | No  |
| Mammalian cell-line          | Cell-based | Imaging        | 1,0E-05           | -3,9           |                | No  |
| Recombinant enzyme           | Binding    | Fluorescence   | 1,0E-05           |                | 4,7            | No  |
| Recombinant enzyme           | Enzymatic  | Absorbance     | 1,0E-05           | -0,1           |                | No  |
| Recombinant enzyme           | Enzymatic  | Fluorescence   | 1,0E-05           | -11,0          |                | No  |
| Recombinant enzyme           | Enzymatic  | Fluorescence   | 1,0E-05           | 1,2            |                | No  |
| Recombinant enzyme           | Enzymatic  | Absorbance     | 5,0E-06           | -2,3           |                | No  |
| CETSA in mammalian cell-line | Cell-based | Luminescence   | 5,0E-05           |                | 19,5           | Yes |
| Recombinant enzyme           | Binding    | Luminescence   | 1,5E-05           | 1,0            |                | No  |
| Recombinant enzyme           | Binding    | Luminescence   | 1,0E-05           | 12,3           |                | No  |

## Supplementary Note 1| Abbreviations

|                        |  |
|------------------------|--|
| CBCS                   | Chemical Biology Consortium Sweden             |
| CDA                    | Cytidine deaminase                             |
| CETSA                  | Cellular thermal shift assay                   |
| DCK                    | Deoxycytidine kinase                           |
| DCTD                   | Deoxycytidylate deaminase                      |
| DMSO                   | Dimethyl sulfoxide                             |
| dUMP                   | 2'-deoxyuridine 5'-monophosphate               |
| EdU                    | 5-ethynyl-2'-deoxyuridine                      |
| EdUMP                  | 5-ethynyl-2'-deoxyuridine 5'-monophosphate     |
| FdU                    | 5-fluoro-2'-deoxyuridine; floxuridine          |
| FdUMP                  | 5-fluoro-2'-deoxyuridine 5'-monophosphate      |
| 5-FU                   | 5-fluorouracil                                 |
| FUR                    | 5-fluorouridine                                |
| HTS                    | High-throughput screening                      |
| ITDRF <sub>CETSA</sub> | Isothermal dose-response fingerprint           |
| LC-MS/MS               | Liquid chromatography-tandem mass spectrometry |
| S.E.M.                 | Standard error of mean                         |
| SPR                    | Surface plasmon resonance                      |

|                  |  |
|------------------|--|
| $T_{\text{agg}}$ | Aggregation temperature                        |
| TFT              | 5-trifluoro-2'-deoxythymidine                  |
| TFTMP            | 5-trifluoro-2'-deoxythymidine 5'-monophosphate |
| TS               | Thymidylate synthase                           |

## Supplementary References

1. Fisher, T. C. *et al.* bcl-2 modulation of apoptosis induced by anticancer drugs: Resistance to thymidylate stress is independent of classical resistance pathways. *Cancer Res.* **53**, 3321–3326 (1993).
2. Jafari, R. *et al.* The cellular thermal shift assay for evaluating drug target interactions in cells. *Nat. Protoc.* **9**, 2100–2122 (2014).
3. Litvinov, V. P. *et al.* New method for the synthesis of substituted 2-pyridones. *Izv. Akad. Nauk SSSR, Ser. Khim.* 1869–1870 (1984).
4. Dyachenko, V. D. *et al.* Cyclization reactions of nitriles. XXXIX. Synthesis and transformations of 6-hydroxy-3-cyano-2(1H)-pyridinechalcogenones. *Zh. Obs. Khim.* **60**, 2384–2392 (1990).
5. Honeywell, R. J., Ruiz van Haperen, V. W. T., Veerman, G., Smid, K. & Peters, G. J. Inhibition of thymidylate synthase by 2',2'-difluoro-2'-deoxycytidine (Gemcitabine) and its metabolite 2',2'-difluoro-2'-deoxyuridine. *Int. J. Biochem. Cell Biol.* **60**, 73–81 (2015).